Highly diastereo- and enantioselective synthesis of trifluoromethyl-substituted cyclopropanes via myoglobin-catalyzed transfer of trifluoromethylcarbene.

Antonio Tinoco, Viktoria Steck, Vikas Tyagi and Rudi Fasan*

Department of Chemistry, University of Rochester, Rochester NY 14620, United States

ABSTRACT: We report on an efficient strategy for the asymmetric synthesis of trifluoromethyl-substituted cyclopropanes by means of myoglobin-catalyzed olefin cyclopropanation reactions in the presence of 2-diazo-1,1,1-trifluoroethane (CF_3CHN_2) as the carbene donor. These transformations were realized using a two-compartment setup in which *ex situ* generated gaseous CF_3CHN_2 is processed by engineered myoglobin catalysts expressed in bacterial cells. This approach was successfully applied to afford a variety of *trans*-1-trifluoromethyl-2-arylcyclopropanes in high yields (61-99%) and excellent diastereo- and enantioselectivity (97-99.9% *de* and *ee*). Furthermore, mirror-image forms of these products could be obtained using myoglobin variants featuring stereodivergent selectivity. These reactions provide a convenient and effective biocatalytic route to the stereoselective synthesis of key fluorinated building blocks of high value for medicinal chemistry and drug discovery. This work expands the range of carbene-mediated transformations accessible via metalloprotein catalysts and introduces a potentially very general strategy for exploiting gaseous and/or hard-to-handle carbene donor reagents in biocatalytic carbene transfer reactions.

Trifluoromethyl-substituted cyclopropanes constitute attractive synthons in medicinal chemistry as they combine the conformational rigidity of three-membered rings with the unique and often highly beneficial features of fluorinated substituents.[1] Reflecting this notion, these structural motifs have represented key building blocks for the design and development of several bioactive molecules and investigational drugs.[1a] Various methods have been investigated to afford these structures, most of which involve starting materials that already incorporate the trifluoromethyl group.[2] A convenient and most direct strategy to access this class of compounds is through the addition of trifluoromethylcarbene to an olefin. Early studies in this area have entailed the use of trifluoromethylcarbene generated by photolytic decomposition of 2-diazo-1,1,1-trifluorethane (CF_3CHN_2), resulting in a mixture of products.[3] More synthetically useful strategies for olefin trifluoromethylcyclopropanation with this reagent were made available only recently using transition metal catalysis.[4] To date, however, only a few studies have addressed the problem of developing enantioselective variants of these transformations.[4a,5] In a first report, Simmoneaux and coworkers described the use of chiral metalloporphyrins for the asymmetric cyclopropanation of styrenes in the presence of 2-diazo-1,1,1-trifluoroethane, but only moderate enantioselectivity (30-79% *ee*) was observed using this system.[4a] Higher selectivity was more recently achieved in similar reactions using Co(III)-salen complexes by Carreira and coworkers.[5] Despite these advances, the development of highly stereoselective strategies for olefin cyclopropanation with 2-diazo-1,1,1-trifluoroethane as the carbene donor remains an outstanding challenge. Here, we report a simple and efficient biocatalytic approach for promoting these transformations that hinges upon the use of engineered myoglobin variants in combination with a compartmentalized reaction setup. This strategy could be applied to the conversion of a broad range of vinylarene substrates, providing access to trifluoromethyl-substituted cyclopropanes with high diastereo- and enantioselectivity as well as stereocomplementary selectivity.

Our group has recently reported the development of engineered myoglobin catalysts for promoting a variety of carbene transfer reactions,[6] including olefin cyclopropanation.[7] These transformations are believed to be mediated by an electrophilic heme-bound carbenoid species generated upon reaction of a diazo compound with the heme cofactor embedded in the protein.[7a] This species can react with a number of nucleophiles (olefins, amines, thiols, phosphines) in order to form new C-C and C-heteroatom bonds, with the protein active site providing an asymmetric environment to affect the stereoselectivity of the carbene transfer process.[6-7] In addition to myoglobin (Mb), other biocatalysts[8] have been investigated for promoting carbene transfer reactions, but the scope of biocatalytic carbene transfer reactions has so far been restricted to α-diazoacetates as carbene donor reagents. Given the high reactivity of myoglobin variants toward the acceptor-only carbene donor reagent ethyl diazoacetate (EDA, **1**), we envisioned that 2-diazo-1,1,1-trifluoroethane (DTE, **2**) could provide a potentially viable carbene precursor for myoglobin-catalyzed cyclopropanations. A well-known challenge associated with the use of DTE in carbene transfer reactions, however, is the difficulty in handling this reagent due to its high toxicity and volatility. *In situ* generation of DTE via diazotization of 2,2,2-trifluoroethylamine has provided an attractive approach for utilizing this reagent in various reaction manifolds,[4c,9] but these conditions are too harsh for protein-based catalysts. To overcome this problem, we envisioned the possibility to utilize a two-compartment reaction setup, in which *ex situ* produced DTE from a 'reagent generation chamber' is carried through a solution containing the myoglobin catalyst by inert gas (**Figure 1**). This system would effectively segregate the two incompatible reactions, thereby preserving the stability of the biocatalyst while eliminating the need for isolating and handling DTE.

To implement this approach, we initially tested the possibility to carry out the myoglobin-catalyzed cyclopropanation of *p*-chloro-styrene (**3**) in the presence of *ex situ* generated EDA. The latter was produced by diazotization of glycine ethyl ester (**4**) in the presence of sodium nitrite and acid (**Table 1**).[10] For these experiments, the Mb(H64V,V64A) variant was chosen as the

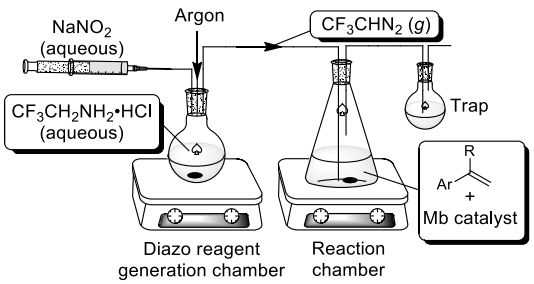

Figure 1. Compartmentalized reaction setup for coupling myoglobin-catalyzed cyclopropanation with *ex situ* generation of 2-diazo-1,1,1-trifluoroethane (DTE).

catalyst based on its high activity and selectivity toward cyclopropanation of aryl-substituted olefins with EDA.[7a] Initial tests involving purified Mb(H64V,V64A) in the reaction chamber produced only small amounts of the cyclopropanation product **6** (**Table 1**, Entry 1), a result we attributed to protein inactivation by the gas stream flowing through the reaction mixture. Given our recent finding that Mb-catalyzed cyclopropanation reactions can be realized using whole cell systems,[7b] a suspension of *E. coli* cells expressing the Mb(H64V,V64A) variant was used as the biocatalytic system in the reaction chamber. Gratifyingly, this modified setup resulted in the accumulation of significantly larger amounts of **6** (**Table 1**, Entry 2). Further improvement of the reaction was possible by varying the cell density of the whole cell transformation and the molar ratio between the olefin substrate and the EDA precursor (**Table 1**, Entries 3-4). Under optimized conditions (i.e., OD_{600} = 40, corresponding to a cell density of ~3.5 g cdw L^{-1}, 10 equivalents of glycine ethyl ester relative to the olefin), nearly quantitative conversion of the *p*-chloro-styrene substrate to **6** was observed within 12 hours (**Table 1**, Entry 5). Importantly, neither the reaction setup nor the whole cell setting was found to have a noticeable impact on the stereoselectivity of the Mb(H64V,V64A)-catalyzed reaction, leading to the formation of the *trans*-(1*S*,2*S*)-configured cyclopropanation product in excellent diastereo- and enantiomeric excess (98.5-99.9% *de*, 99.8-99.9% *ee*).

Based on these promising results, we next investigated the possibility to supply the Mb catalyst in the whole cell system with gaseous DTE as the carbene donor. In this case, 2,2,2-trifluoroethylamine (**5**) was subjected to the diazotization reaction in the reagent generation chamber (**Table 1**). To our delight, excellent conversion of *p*-chloro-styrene to the desired trifluoromethyl-substituted cyclopropane **7b** (92%) was observed in less than five hours (Entry 7, **Table 1**) and using only 5 equivalents of the diazo reagent precursor **5**. Because of the higher volatility of **7b** compared to **6**, product recovery in this case was improved by addition of a water trap downstream of the reaction vessel. No product was detected using cells not expressing the Mb variant, thus demonstrating the direct role of the hemoprotein in mediating the carbene transfer reaction. Under the applied conditions, the Mb variant was estimated to support about 520 catalytic turnovers (TON), as determined based the hemoprotein concentration in the reaction mixture measured via a CO-binding assay. This TON value is higher than that observed in the presence of *ex situ* generated EDA under identical operational conditions (Entry 7 vs. 3, **Table 1**). Higher yields (GC) and TON were also observed in the presence of DTE vs. EDA when purified Mb(H64V,V64A) was applied as the catalyst (Entry 6 vs. 1). These differences are likely to reflect the inherent reactivity of the diazo reagents as well as differences in the rate and efficiency with which the *ex situ* generated reagents are transferred from the generation chamber to the reaction vessel (**Figure 1**). Importantly, Mb(H64V,V68A)-catalyzed synthesis of **7b** was found to occur with excellent diastereo- and enantioselectivity (99.9% *de* and *ee*).

Table 1. Mb(H64V,V68A)-catalyzed cyclopropanation of *p*-chlorostyrene in the presence of *ex situ* generated EDA and DTE.[a]

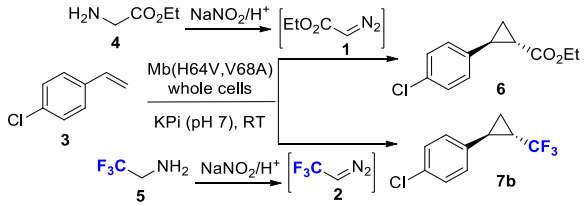

Entry	Catal.	Prod.	Equiv **4** or **5** [b]	Yield[c]	TON	% *de*	% *ee*
1	protein	**6**	2	4%	180	99.9	99.8
2	cells[d]	**6**	2	47%	560	97.2	99.9
3	cells	**6**	5	80%	365	99.9	99.8
4	cells	**6**	10	75%	340	98.5	99.9
5	cells	**6**	10	>99%[e]	500	99.9	99.9
6	protein	**7b**	5	22%	1,110	98.5	99.9
7	cells	**7b**	5	92% (67%)	520	99.9	99.9

[a] Reactions were carried out at a 20 mL-scale with 30 mM 4-chloro-styrene (**3**), purified Mb variant (20 μM) or Mb(H64V,V68A)-expressing *E. coli* (BL21(DE3)) cells (OD_{600} = 40) in KPi 50 mM (pH 7), RT, 5 hours. Diazo reagent was supplied using indicated equivalents of **4** or **5** (slow addition over 4 hours). [b] Relative to olefin. [c] As determined by GC using calibration curves generated with isolated product as reference. Isolated yields are reported in parentheses. [d] OD_{600} = 20. [e] Reaction time: 12 hours.

To explore the scope of this reaction, a series of styrene derivatives and aryl-substituted olefins was investigated. As shown by the data in **Table 2**, all of these substrates could be efficiently converted to the corresponding trifluoromethyl-containing cyclopropanes (54-99%) using Mb(H64,V68A)-expressing cells in the two-compartment setup described in **Figure 1**. These included *meta*- and *para*-substituted styrene derivatives containing both electron-donating and electron-withdrawing groups. 4-Nitrostyrene displayed lower reactivity toward Mb-catalyzed cyclopropanation than electronrich styrene derivatives (e.g., products **9b**, **11b**, **12b**), a result consistent with the electrophilic character of the putative heme-carbenoid intermediate expected to mediate these reactions.[7a] As demonstrated by the results with **13b** and **14b**, the Mb-catalyzed transformation could be readily extended to other aryl-substituted olefins such as 2-vinyl-naphthalene and 3-(propen-2-yl)thiophene, supporting the broad substrate scope of the Mb(H64,V64A) variant. In contrast to protocols involving chiral metalloporphyrins,[4a] the biocatalytic reactions proceed efficiently using the olefin as the limiting reagent, which increases their attractiveness for the transformation of valuable starting materials. Importantly, using Mb(H64V,V68A)-expressing cells, the cyclopropanation prod-

uct was afforded in most cases with high diastereosteroselectivity (99.9% *de*) and enantioselectivity (92-99.9% *ee*). As an exception, moderate enantioselectivity (28-31% *ee*) was observed with the toluene derivatives **11a** and **12a** (**Table 2**, Entries 4-5). For these compounds, however, excellent diastereo- and enantioselectivity (97-99.9% *de* and *ee*) could be achieved using cells expressing Mb(H64V,V68G), a Mb variant previously identified as having similar selectivity properties to Mb(H64V,V68A) in cyclopropanation reactions with EDA.[7b] Altogether, the stereoselectivity offered by these Mb-based catalysts exceeds those provided by the most selective synthetic catalysts reported to date for the asymmetric synthesis of related CF_3-containing cyclopropanes (84-91% *ee*).[5] Compared to the latter, the Mb-catalyzed transformations also involve shorter reaction times (5 vs. 14 hours) and higher catalytic efficiency (e.g., 520 vs. ~10 TON for **7b**). The use of whole cells bypasses the need for purification and isolation of the myoglobin catalyst, which further simplifies the overall procedure from a technical standpoint. From these reactions, the CF_3-substituted cyclopropane products could be isolated in good yields (43-82%, **Table 2**). The synthetic utility of these transformations was further evidenced by a larger scale reaction with *p*-methoxy-styrene, from which 0.1 g of **9b** was obtained in 76% isolated yield and excellent diastereo- and enantiomeric excess (99.9% *de*, 99.9% *ee*).

Table 2. Substrate scope of myoglobin-catalyzed olefin cyclopropanation with *ex situ* generated DTE.[a]

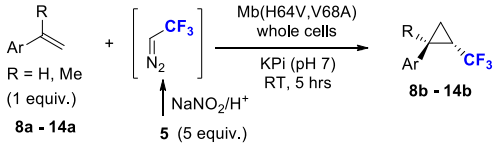

Entry	Product	OD_{600}	Yield [b]	% *de*	% *ee*
1	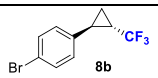 **8b**	80	69% (68%)	99.9	99.9
2	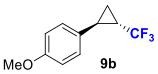 **9b**	80	92% (76%)	99.9	99.9
3	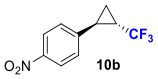 **10b**	80	54% (43%)	99.9	99.9
4	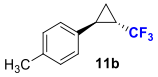 **11b**	40 80	85% 88% (78%)	96 96 [c]	31 97 [c]
5	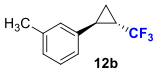 **12b**	40 80	76% >99% (82%)	99.8 99.9 [c]	28 99.9 [c]
6	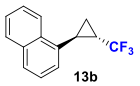 **13b**	80	70% (58%)	99.9	92
7	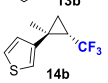 **14b**	40	>99% (71%)	99.9	99.9

[a] Reactions were carried out at 20 mL-scale with Mb(H64V,V68A)-expressing *E. coli* at indicated cell density, 8-30 mM olefin in KPi 50 mM (pH 7), room temperature, 5 hours. DTE was supplied using 5 equiv. **5** (slow addition over 4 hours). [b] As determined by GC using calibration curves generated with isolated product as reference. Isolated yields are reported in parentheses. [c] Using cells expressing Mb(H64V,V68G).

To elucidate the stereoselectivity of the Mb(H64V,V68A) catalyst in these reactions, product **10b** was crystallized and determined to have a *trans*-(1*S*,2*S*) configuration by X-ray diffraction analysis (**Figure 2A**). The same configuration was indirectly assigned to **7b** and the other cyclopropanation products of **Table 2** based on the similar order of elution for the corresponding enantiomers upon resolution via chiral GC or SFC (see **Figure S2**). The stereoselectivity of Mb(H64V,V68A) in the cyclopropanation reactions with DTE thus mirrors that observed in the reactions with EDA.[7a] Leveraging this insight and in consideration of the structural and electronic similarities between EDA and DTE, we propose a stereochemical scenario analogous to that proposed for Mb(H64V,V68A)-catalyzed cyclopropanation of aryl-substituted olefins with EDA[7a]. Specifically, the 'cavity' created by the Val68→Ala substitution (**Figure S1**) is expected to facilitate orientation of the bulkier $-CF_3$ group (cp. to $-H$) in the heme-bound carbene intermediate in proximity to the N2 atom of the heme cofactor (**Figure 2B**). This active site configuration enforces high facial selectivity during end-on attack of the olefin to this reactive species, giving rise to the observed *trans*-(1*S*,2*S*)-configured product. Consistent with this scenario, the Mb(H64V,V68G) variant, which features a similar 'large-to-small' mutation at position 68 (**Figure S1**), is also *trans*-(1*S*,2*S*) selective (**Table 2,** Entries 4-5). An implication of the proposed model is that the aryl ring of the olefin projects toward the solvent-exposed side of the active site, a molecular arrangement that is consistent with Mb(H64V,V68A) ability to process structurally diverse vinylarene substrates with consistently high *trans*-(1*S*,2*S*) selectivity (**Table 2**).

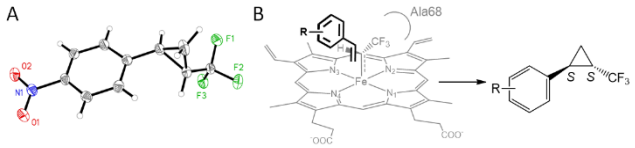

Figure 2. A) Crystal structure of (1*S*,2*S*)-2-(trifluoromethyl)cyclopropyl)-4-nitro-benzene product (**10b**). B) Plausible geometry for vinylarene attack to heme-bound trifluoromethylcarbene intermediate leading to the (1*S*,2*S*)-configured cyclopropane product.

Given the parallelism between the stereoselectivity exhibited by Mb(H64V,V68A) with EDA and DTE, we surmised that the stereoselectivity of Mb variants in cyclopropanation reactions with EDA could serve as a general predictor for their stereoselectivity in the cyclopropanation of related substrates with DTE. Supporting this notion, a very good correlation (R^2 = 0.911) was found between the enantiomeric excess exhibited by a series of active site Mb variants in the cyclopropanation of *p*-methoxy-styrene with EDA vs. that of parallel reactions with DTE as the carbene donor (**Figure 3A**). In addition to Mb(H64V,V68A), this panel comprised other Mb variants with high *trans*-(1*S*,2*S*)-selectivity (Mb(H64V,V68G), Mb(H64V,V68S)) as well as a series of recently developed Mb catalysts with high *trans*-(1*R*,2*R*)-selectivity in olefin cyclopropanation with EDA (variants RR1 through RR5).[7b] Mb variants that span a range of enantioselectivity values from 13% *ee* (wild-type Mb) to 86% *ee* (Mb(V68A)) in the latter reaction were included as additional references (**Table S1**). As illustrated by the data of **Figure 3A** and **Table S1**, the diastereo- and enantioselectivity of the trifluoromethylcarbene transfer reaction was found to closely mirror the diastereo- and enantioselectivity of these Mb variants in the α-diazoester carbene transfer reaction (average $|\Delta(de)| = 3.3\%$; average $|\Delta(ee)| = 14.4\%$; **Table S1**). Based on these analyses, RR2 (= Mb(H64V,V68L,L29T)) was selected as a promising candidate for gaining access to the mirror-image forms of products **7b-14b**. Gratifyingly, reactions with RR2-expressing

E. coli cells produced the desired *trans*-(1*R*,2*R*) trifluoromethyl-substituted cyclopropanes **7c**-**14c** with excellent diastereoselectivity (98% *de* for **9c**, >99.5% *de* for the others) and high enantioselectivity (80-92% *ee*; **Figure 3B; Figure S2**). As an exception, **13c** was obtained only in 21% *ee*. However, this compound could be synthesized in higher enantiomeric excess (58% *ee*) using RR4, as anticipated by the high *trans*-(1*R*,2*R*)-selectivity of this Mb variants in olefin cyclopropanation with EDA (**Figure 3A**). Altogether, these experiments demonstrate the versatility of the Mb scaffold toward providing access to both enantiomeric forms of the target trifluoromethyl-containing cyclopropanes. They also support the predictable reactivity of these biocatalysts in the presence of structurally and electronically related carbene donors.

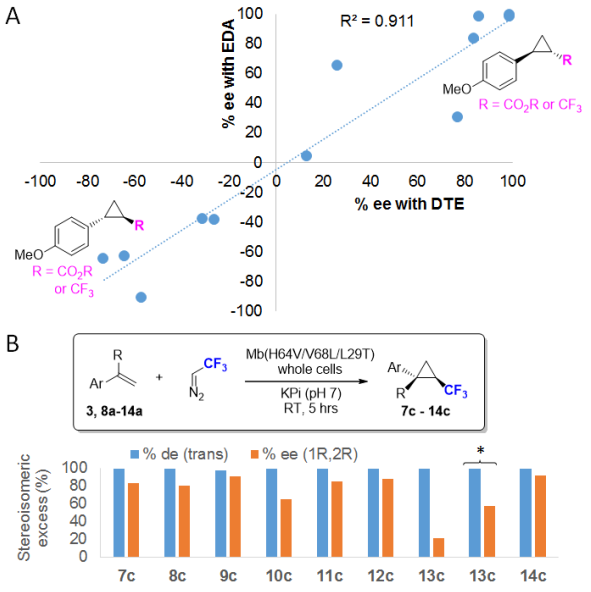

Figure 3. Stereocomplementary selectivity. A) Correlation between enantioselectivity of Mb variants (n = 12) in cyclopropanation of *p*-methoxy-styrene with EDA vs. DTE. See **Table S1** for additional data. B) Diastereo- and enantioselectivity of *trans*-(1*R*,2*R*)-selective Mb variant RR2 in cyclopropanation of aryl-substituted olefins in the presence of DTE. See **Table S2** for details. * = with RR4-expressing cells.

In summary, we have developed a biocatalytic strategy for the asymmetric synthesis of trifluoromethyl-substituted cyclopropanes via myoglobin-catalyzed addition of trifluoromethylcarbene to olefins. These transformations could be applied to a variety of vinylarene substrates, offering unprecedented levels of diastereo- and enantioselectivity. Furthermore, both enantiomers of the target CF_3-containing products could be accessed using Mb catalysts with complementary stereoselectivity, whose choice was guided by their reactivity with EDA. The reactions presented here provide access to enantioenriched fluorinated building blocks of high value for medicinal chemistry. This study provides a first-time demonstration that carbene donor reagents other than α-diazoesters can be engaged in biocatalytic carbene transfer reactions. This finding, combined with the demonstrated feasibility of coupling these reactions with *ex situ* generated diazo compounds, is anticipated to enable extension of the present approach to a variety of other carbene precursors in order to expand the scope of carbene-mediated transformations accessible with myoglobins and other metalloprotein catalysts. Further studies in this direction are currently underway in our laboratory.

ASSOCIATED CONTENT

Supporting Information

Supporting information includes Supplementary Tables and Figures, experimental procedures, compound characterization data andcrystallographic data.

AUTHOR INFORMATION

Corresponding Author

* rfasan@ur.rochester.edu

ACKNOWLEDGMENT

This work was supported in part by the U.S. National Institute of Health grant GM098628 and in part by the National Science Foundation grant CHE-1609550. The authors are grateful to Dr. William Brennessel (U. Rochester) and Dr. Eric Reinheimer (Rigaku Oxford Diffraction) for assistance with crystallographic analyses.

REFERENCES

(1) (a) Grygorenko, O. O.; Artamonov, O. S.; Komarov, I. V.; Mykhailiuk, P. K. *Tetrahedron* **2011**, *67*, 803; (b) Bos, M.; Poisson, T.; Pannecoucke, X.; Charette, A. B.; Jubault, P. *Chem. Eur. J.* **2017**, *23*, in press (doi: 10.1002/chem.201604564).

(2) (a) Katagiri, T.; Yamaji, S.; Handa, M.; Irie, M.; Uneyama, K. *Chem. Commun.* **2001**, 2054; (b) Wang, Y.; Zhao, X. M.; Li, Y. H.; Lu, L. *Tetrahedron Lett.* **2004**, *45*, 7775; (c) Risse, J.; Fernandez-Zumel, M. A.; Cudre, Y.; Severin, K. *Org. Lett.* **2012**, *14*, 3060; (d) Duncton, M. A. J.; Singh, R. *Org. Lett.* **2013**, *15*, 4284; (e) Zhu, C. L.; Yang, L. J.; Li, S.; Zheng, Y.; Ma, J. A. *Org. Lett.* **2015**, *17*, 3442.

(3) Atherton, J. H.; Fields, R. *J. Chem. Soc. C* **1967**, 1450.

(4) (a) Le Maux, P.; Juillard, S.; Simonneaux, G. *Synthesis* **2006**, 1701; (b) Mykhailiuk, P. K.; Afonin, S.; Ulrich, A. S.; Komarov, I. V. *Synthesis* **2008**, 1757; (c) Morandi, B.; Carreira, E. M. *Angew. Chem. Int. Ed.* **2010**, *49*, 4294.

(5) Morandi, B.; Mariampillai, B.; Carreira, E. M. *Angew. Chem. Int. Ed.* **2011**, *50*, 1101.

(6) (a) Sreenilayam, G.; Fasan, R. *Chem. Commun.* **2015**, *51*, 1532; (b) Tyagi, V.; Bonn, R. B.; Fasan, R. *Chem. Sci.* **2015**, *6*, 2488; (c) Tyagi, V.; Fasan, R. *Angew. Chem. Int. Ed.* **2016**, *55*, 2512; (d) Tyagi, V.; Sreenilayam, G.; Bajaj, P.; Tinoco, A.; Fasan, R. *Angew. Chem. Int. Ed.* **2016**, *55*, 13562.

(7) (a) Bordeaux, M.; Tyagi, V.; Fasan, R. *Angew. Chem. Int. Ed.* **2015**, *54*, 1744; (b) Bajaj, P.; Sreenilayam, G.; Tyagi, V.; Fasan, R. *Angew. Chem. Int. Ed.* **2016**, *55*, 16110.

(8) (a) Coelho, P. S.; Brustad, E. M.; Kannan, A.; Arnold, F. H. *Science* **2013**, *339*, 307; (b) Renata, H.; Wang, Z. J.; Kitto, R. Z.; Arnold, F. H. *Catal. Sci. Technol.* **2014**, *4*, 3640; (c) Wang, Z. J.; Renata, H.; Peck, N. E.; Farwell, C. C.; Coelho, P. S.; Arnold, F. H. *Angew. Chem. Int. Ed.* **2014**, *53*, 6810; (d) Weissenborn, M. J.; Low, S. A.; Borlinghaus, N.; Kuhn, M.; Kummer, S.; Rami, F.; Plietker, B.; Hauer, B. *Chemcatchem* **2016**, *8*, 1636; (e) Srivastava, P.; Yang, H.; Ellis-Guardiola, K.; Lewis, J. C. *Nat. Commun.* **2015**, *6*, 7789; (f) Dydio, P.; Key, H. M.; Nazarenko, A.; Rha, J. Y.; Seyedkazemi, V.; Clark, D. S.; Hartwig, J. F. *Science* **2016**, *354*, 102; (g) Key, H. M.; Dydio, P.; Clark, D. S.; Hartwig, J. F. *Nature* **2016**, *534*, 534; (h) Rioz-Martinez, A.; Oelerich, J.; Segaud, N.; Roelfes, G. *Angew. Chem. Int. Ed.* **2016**, *55*, 14136.

(9) (a) Morandi, B.; Carreira, E. M. *Angew. Chem. Int. Ed.* **2010**, *49*, 938; (b) Morandi, B.; Carreira, E. M. *Angew. Chem. Int. Ed.* **2011**, *50*, 9085; (c) Hyde, S.; Veliks, J.; Liegault, B.; Grassi, D.; Taillefer, M.; Gouverneur, V. *Angew. Chem. Int. Ed.* **2016**, *55*, 3785.

(10) (a) Barrett, A. G. M.; Braddock, D. C.; Lenoir, I.; Tone, H. *J. Org. Chem.* **2001**, *66*, 8260; (b) Wurz, R. P.; Charette, A. B. *Org. Lett.* **2002**, *4*, 4531.

Supporting Information for

Highly diastereo- and enantioselective synthesis of trifluoromethyl-substituted cyclopropanes via myoglobin-catalyzed transfer of trifluoromethylcarbene.

Antonio Tinoco, Viktoria Steck, Vikas Tyagi and Rudi Fasan*

Department of Chemistry, University of Rochester, 14627 Rochester, New York, USA

Correspondence should be addressed to R.F. (rfasan@ur.rochester.edu)

Table of contents:

Table S1. Diastereo- and enantioselectivity of Mb variants in whole-cell cyclopropanation of *p*-methoxystyrene in the presence of EDA or *ex situ* generated DTE. The absolute difference for the % *de* and % *ee* values measured with the two different carbene donors is also indicated. The graph in **Figure 3A** was generated by plotting the % *ee* values with EDA vs % *ee* value with DTE and by fitting the data with a linear regression model.

Mb Variant	*p*-methoxy-styrene + EDA [a]		*p*-methoxy-styrene + DTE [b]		|Δ(%*de*)|	|Δ(%*ee*)|
	% *de* (trans)	% *ee* (1*S*,2*S*)	% *de* (trans)	% *ee* (1*S*,2*S*)		
WT	79	13	70	4	9	9
Mb(H64V)	91	26	>99	65	8	39
Mb(V68A)	97	86	>99	98	2	12
Mb(H64V,V68A)	>99	99	>99	99.5	0	0.5
Mb(H64V,V68S)	98	84	97	83	1	1
Mb(H64V,V68G)	93	99	>99	98	6	1
Mb(H64V,I107W)	93	77	93	30	0	47
Mb(H64V,V68F,L29S) (= RR1)	89	-64	90	-63	1	1
Mb(H64V,V68L,L29T) (= RR2)	96	-57	98	-91	2	34
Mb(H64V,V68F,L29T) (= RR3)	97	-26	92	-39	5	13
Mb(H64V,V68F,L29T,I107L) (= RR4)	96	-73	94	-65	2	8
Mb(H64V,V68F,L29T,F43W) (= RR5)	89	-31	93	-38	4	7

[a] Reaction conditions: 400 µL scale reactions using 10 mM 4-methoxy-styrene (**9a**), 20 mM ethyl diazoacetate (EDA), and 380 µL *E. coli* (C41(DE3)) cells (OD_{600} = 40) expressing the indicated Mb variant in phosphate buffer (pH 7.2), room temp., 16 hours.

[b] Reaction conditions: 10 mL scale using 10 mM 4-methoxy-styrene (**9a**), 4 equiv. trifluoroethylamine (**5**) and 9.5 mL *E. coli* (C41(DE3)) cells (OD_{600} = 40) expressing the indicated Mb variant in phosphate buffer (pH 7.2), room temp., 16 hours.

Table S2. Diastereo- and enantioselectivity of *trans*-(1*R*,2*R*)-selective Mb variant RR2 (and RR4) for cyclopropanation of aryl-substituted olefins in the presence of *ex situ* generated DTE. Reactions were carried out on a 10 mL scale using Mb(H64V,V68L,L29T)-expressing *E. coli* (C41(DE3)) cells (OD_{600} = 40), 7.5 mM olefin, 4 equiv. trifluoroethylamine (**5**) in phosphate buffer (pH 7.2), room temp., 2.5 hours. [a] using OD_{600} = 80. [b] using 15 mM substrate. [c] using 12 equiv. trifluoroethylamine (**5**). [d] 5 hours.

Entry	Substrate	Product	Mb variant	% *de* (trans)	% *ee* (1*R*,2*R*)
1	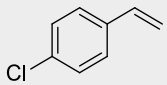 **7a**	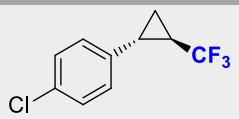 **7c**	Mb(H64V,V68L,L29T) = RR2	99.9	83
2	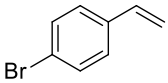 **8a**	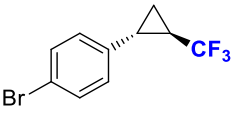 **8c**	Mb(H64V,V68L,L29T) = RR2	99.9	80
3	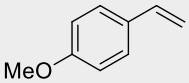 **9a**	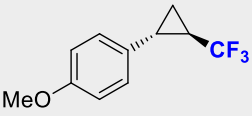 **9c**	Mb(H64V,V68L,L29T) = RR2	98	91
4	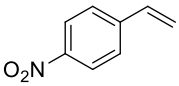 **10a**	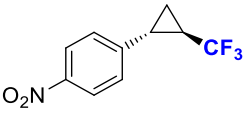 **10c**	Mb(H64V,V68L,L29T) = RR2	99.9	65
5[a,b]	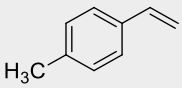 **11a**	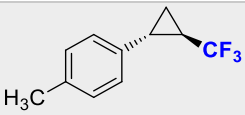 **11c**	Mb(H64V,V68L,L29T) = RR2	99.9	85
6[a,b]	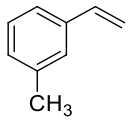 **12a**	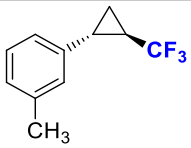 **12c**	Mb(H64V,V68L,L29T) = RR2	99.9	88
7[a,c]	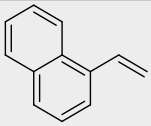 **13a**	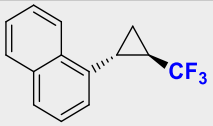 **13c**	Mb(H64V,V68L,L29T) = RR2 Mb(H64V,V68L,L29T,I107L) = RR4	99.9 99.9	21 58
8[a,c]	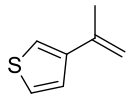 **14a**	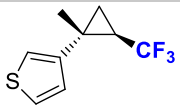 **14c**	Mb(H64V,V68L,L29T) = RR2	99.9	92

Figure S1. Impact of Val68 mutations on active site configuration in myoglobin. (a) Ribbon representation of wild-type sperm whale myoglobin (pdb 1A6K) ; (b) close-up view of the heme distal pocket, showing the heme cofactor (tan) and amino acid residues defining the active site (orange) as stick models; (c) top views of the heme pocket in wild-type myoglobin (*left*) and models of this protein after substitution of Val68 with alanine (*middle*) or glycine (*right*). The latter highlight the cavity created by the V68A/G mutations (yellow) in proximity of pyrrole atom N2 (labeled) of the heme group, which is proposed to favor orientation of the heme-bound trifluoromethylcarbene group as depicted in **Figure 2A**.

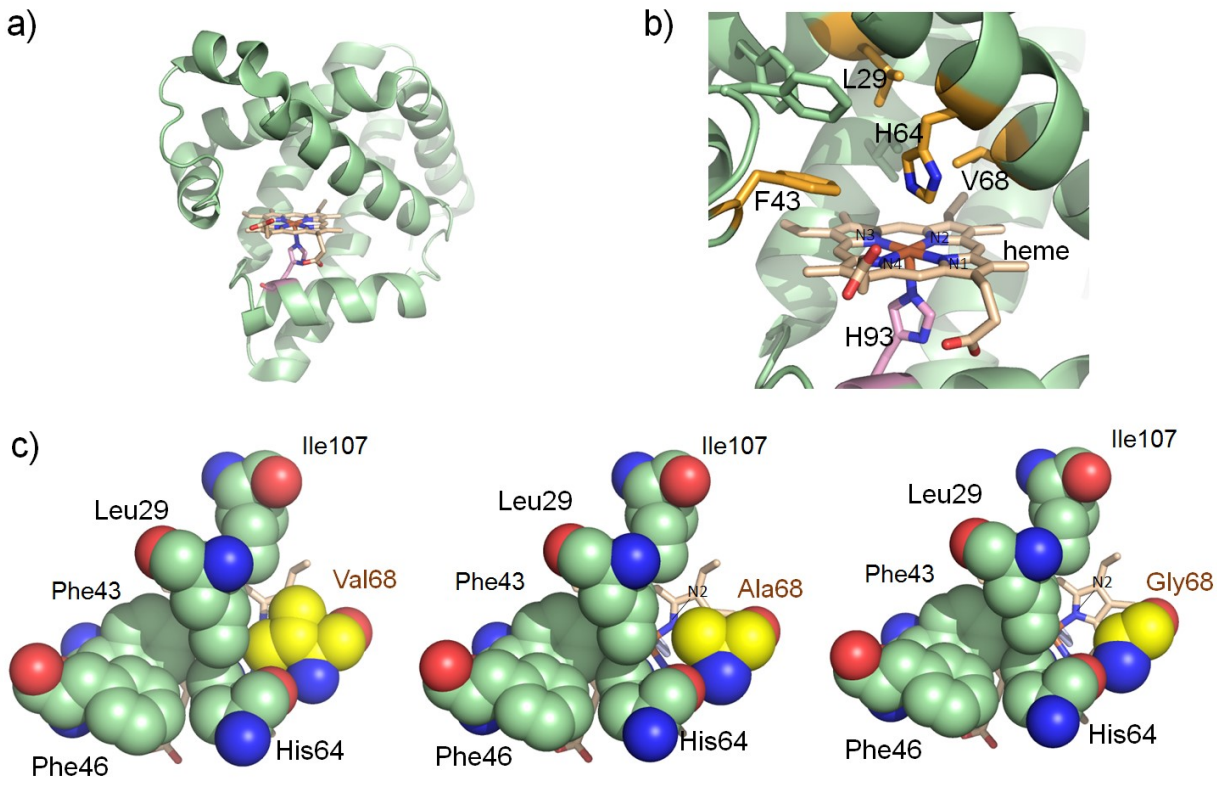

Figure S2. Chiral GC and SFC chromatograms for determination of enantiomeric excess in the cyclopropanation reactions catalyzed by the Mb variants. Reference racemic samples were prepared using Fe(III)(TPP)Cl catalyst as described in the experimental procedures.

(a) Reaction with 4-chloro-styrene (**7a**) and DTE to give **7b-c**:

i. Chiral GC analysis of Fe(III)(TPP)Cl-catalyzed reaction:

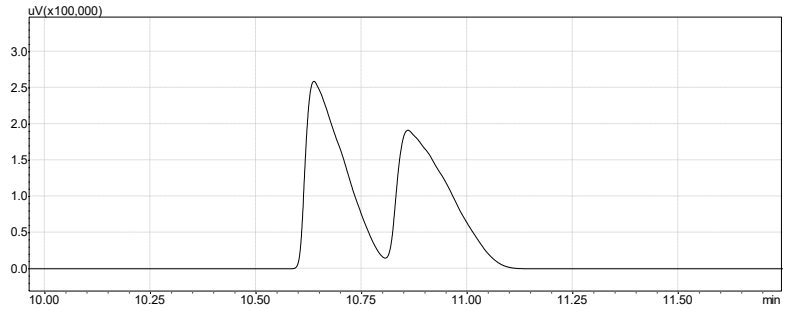

ii. Chiral GC analysis of Mb(H64V,V68A)-catalyzed reaction:

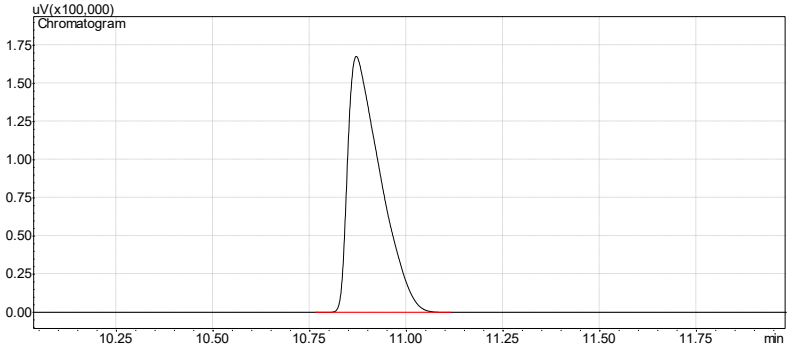

iii. Chiral GC analysis of RR2 (=Mb(H64V,V68L,L29T))-catalyzed reaction:

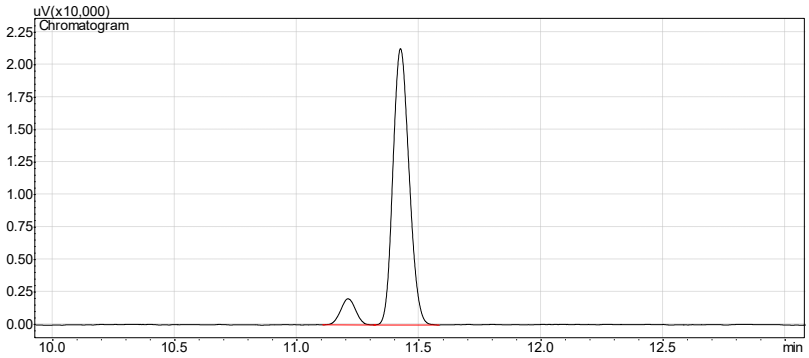

(b) Reaction with 4-bromo-styrene (**8a**) and DTE to give **8b-c**:

i. Chiral GC analysis of Fe(III)(TPP)Cl-catalyzed reaction:

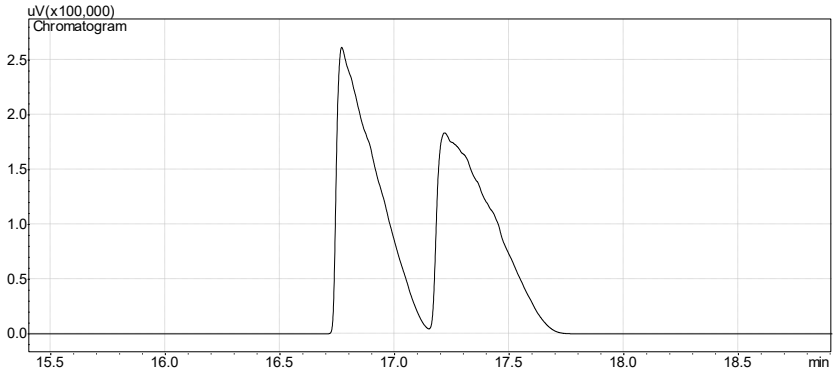

ii. Chiral GC analysis of Mb(H64V,V68A)-catalyzed reaction:

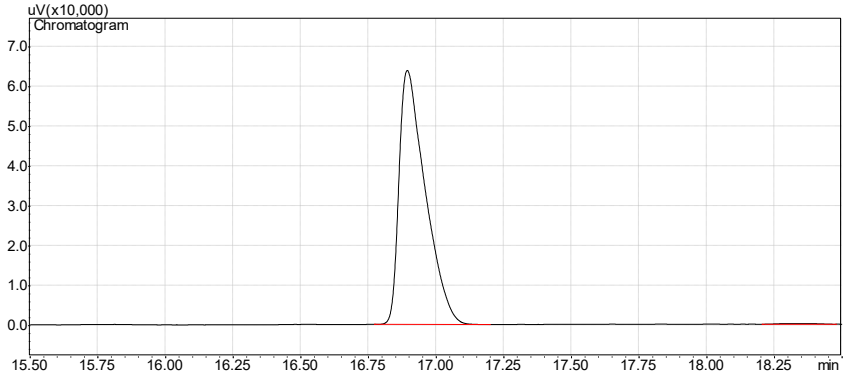

iii. Chiral GC analysis of RR2-catalyzed reaction:

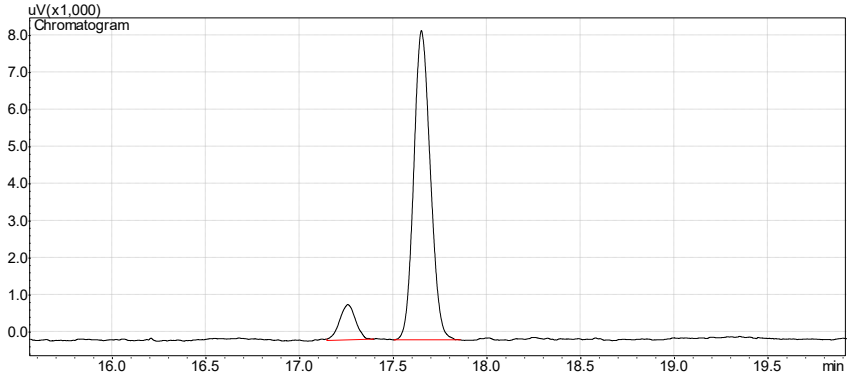

(c) Reaction with 4-methoxy-styrene (**9a**) and DTE to give **9b-c**:

i. Chiral GC analysis of Fe(III)(TPP)Cl-catalyzed reaction:

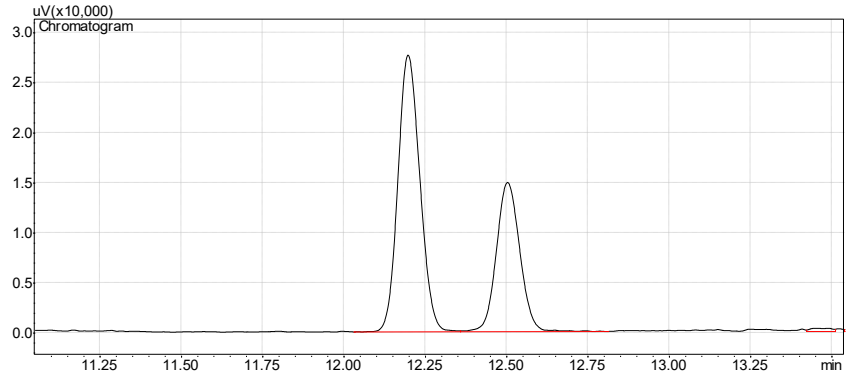

ii. Chiral GC analysis of Mb(H64V,V68A)-catalyzed reaction:

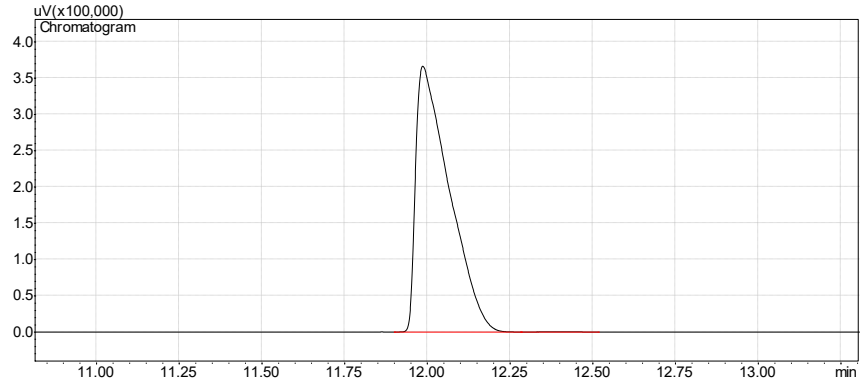

iii. Chiral GC analysis of RR2-catalyzed reaction:

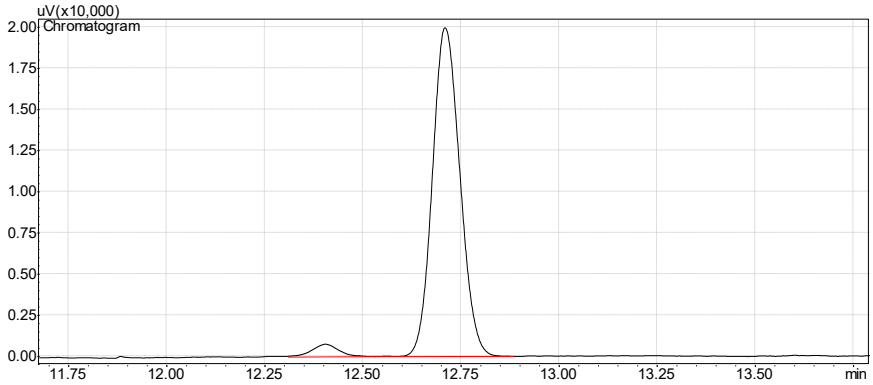

(d) Reaction with 4-nitro-styrene (**10a**) and DTE to give **10b-c**:

i. Chiral GC analysis of Fe(III)(TPP)Cl-catalyzed reaction:

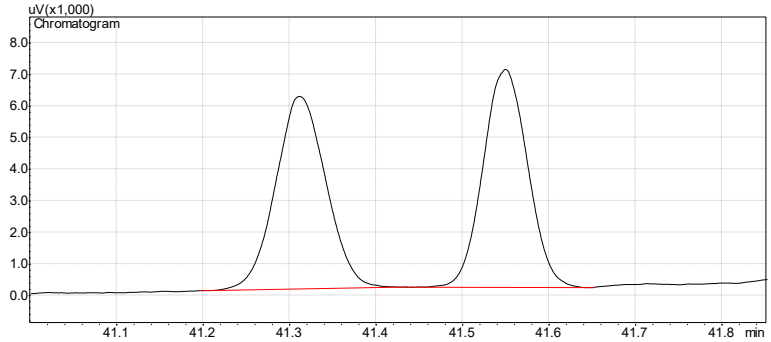

ii. Chiral GC analysis of Mb(H64V,V68A)-catalyzed reaction:

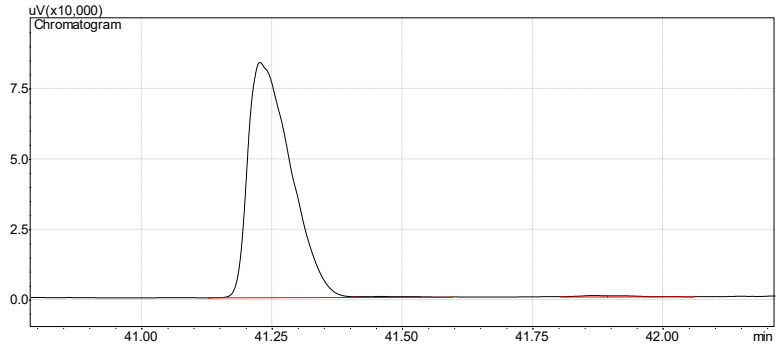

iii. Chiral GC analysis of RR2-catalyzed reaction:

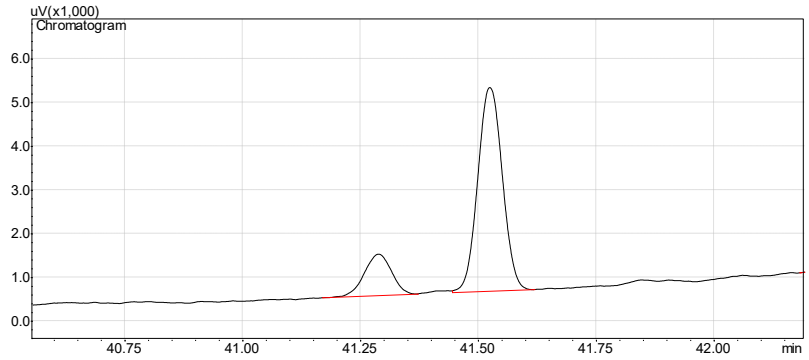

(e) Reaction with 4-methyl-styrene (**11a**) and DTE to give **11b-c**:

i. Chiral GC analysis of Fe(III)(TPP)Cl-catalyzed reaction:

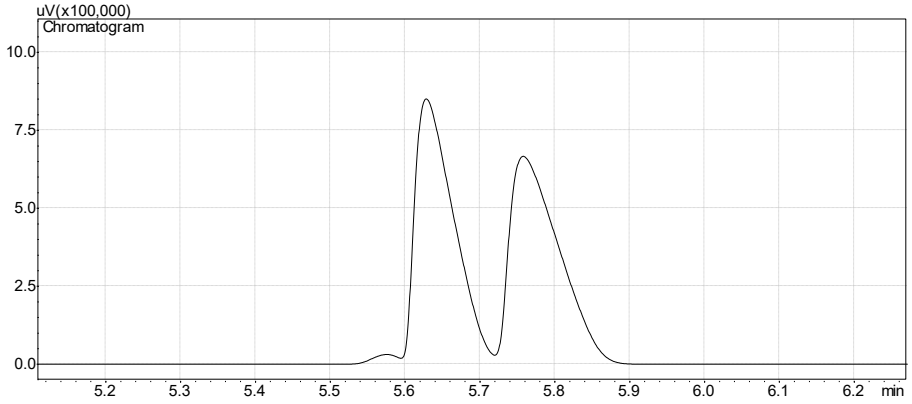

ii. Chiral GC analysis of Mb(H64V,V68G)-catalyzed reaction:

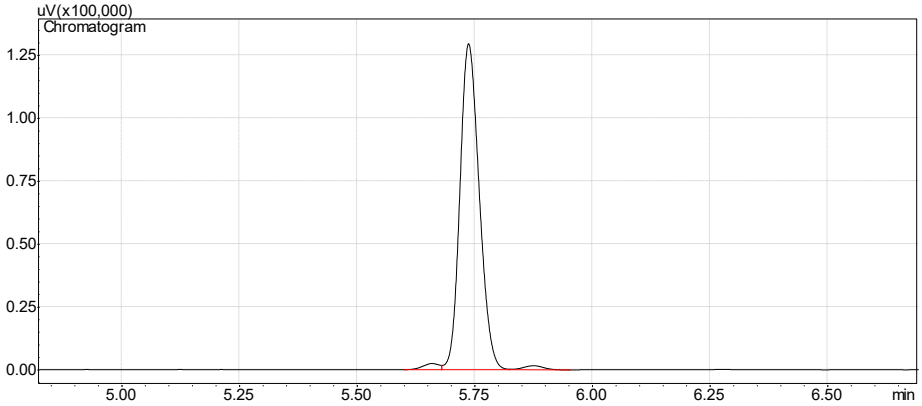

iii. Chiral GC analysis of RR2-catalyzed reaction:

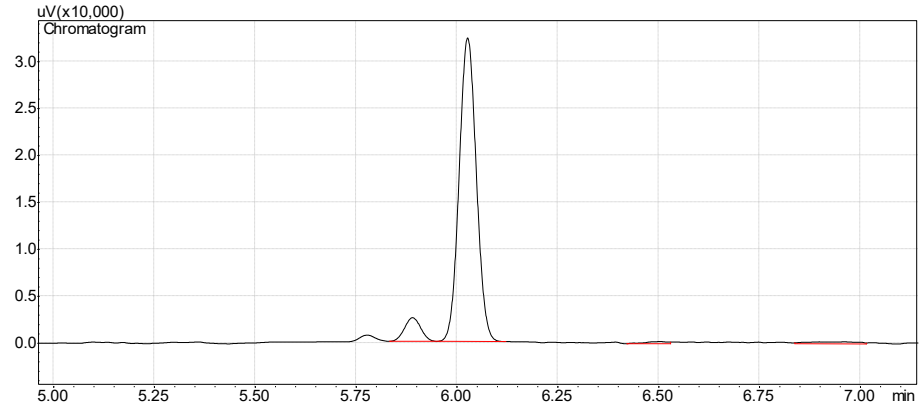

(f) Reaction with 3-methyl-styrene (**12a**) and DTE to give **12b-c**:

i. Chiral GC analysis of Fe(III)(TPP)Cl-catalyzed reaction:

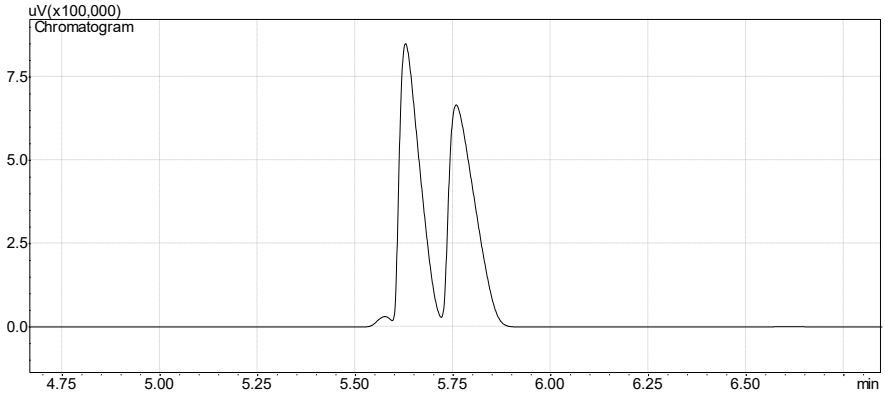

ii. Chiral GC analysis of Mb(H64V,V68G)-catalyzed reaction:

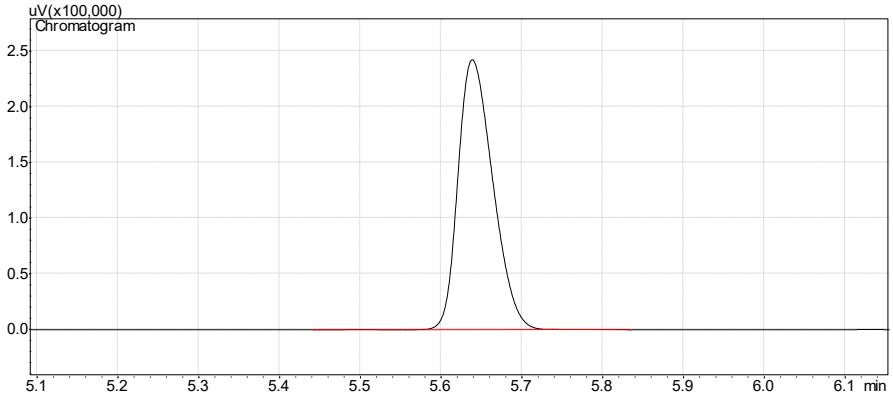

iii. Chiral GC analysis of RR2-catalyzed reaction:

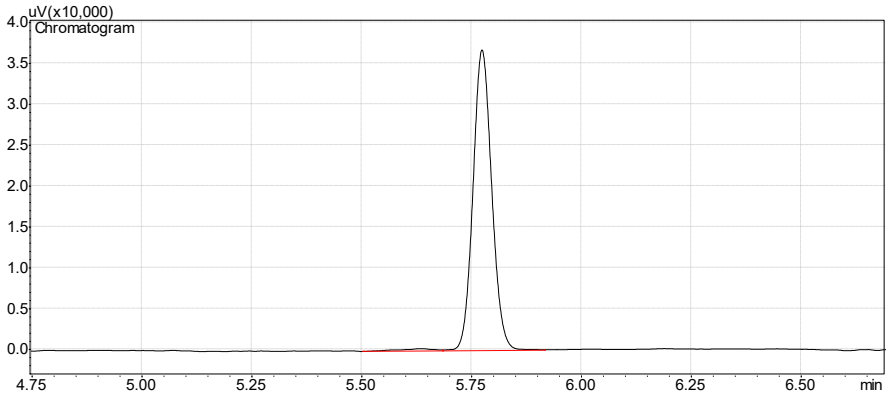

(g) Reaction with 1-vinyl-naphtalene (**13a**) and DTE to give **13b-c**:

i. Chiral SFC analysis of Fe(III)(TPP)Cl-catalyzed reaction:

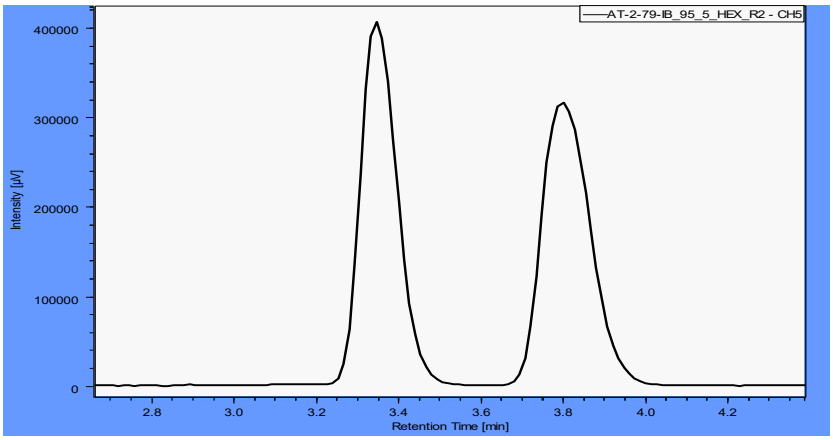

ii. Chiral SFC analysis of Mb(H64V,V68A)-catalyzed reaction:

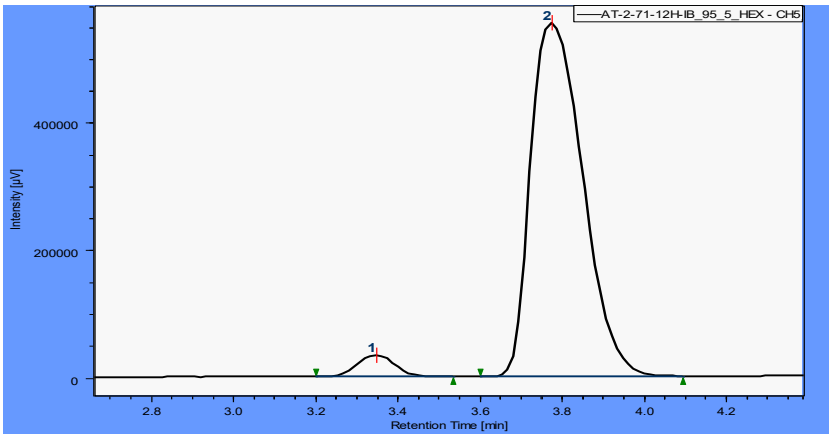

iii. Chiral SFC analysis of RR4-catalyzed reaction:

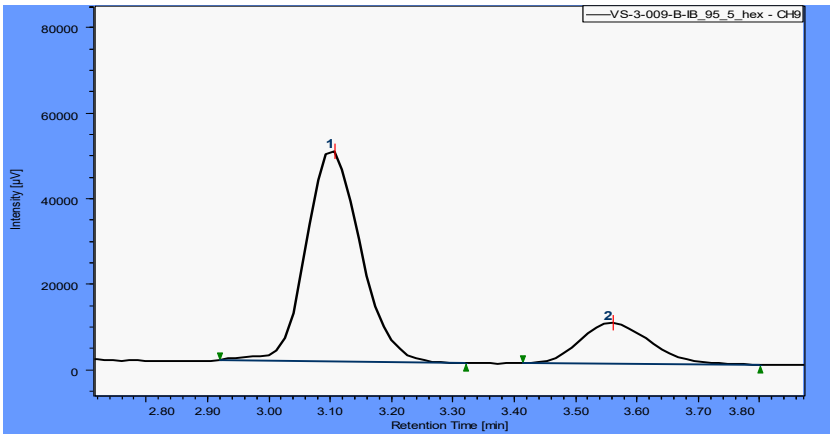

(h) Reaction with 3-(prop-1-en-2-yl)thiophene (**14a**) and DTE to give **14b-c**:

i. Fe(III)(TPP)Cl-catalyzed reaction:

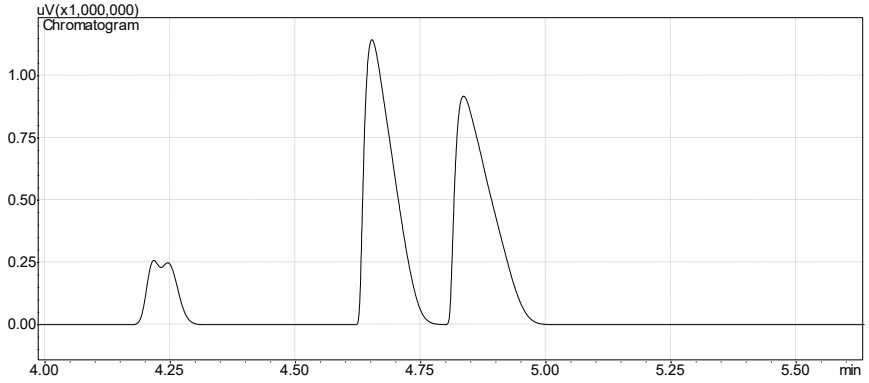

ii. Mb(H64V,V68A)-catalyzed reaction:

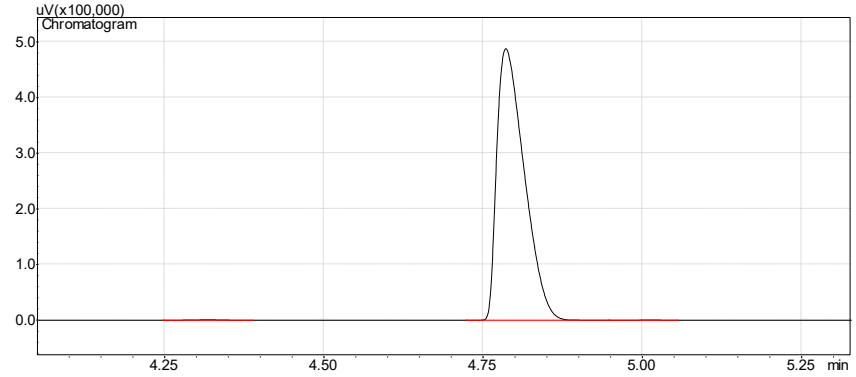

iii. RR2 (=Mb(H64V,V68L,L29T))-catalyzed reaction:

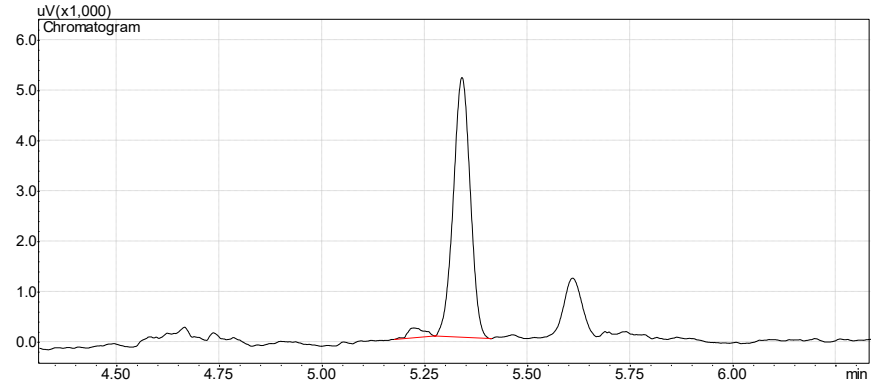

Experimental Procedures

General Information

All chemicals and reagents were purchased from commercial suppliers (Sigma-Aldrich, ACS Scientific, Alfa Aeser, J.T. Baker) and used without any further purification, unless otherwise stated. All reactions were carried out under argon pressure in oven-dried glassware with magnetic stirring using standard gas-tight syringes, cannulae, and septa. ^{1}H, ^{13}C, and ^{19}F NMR spectra were measured on a Bruker DPX-400 instrument (operating at 400 MHz for ^{1}H, 100 MHz for ^{13}C, and 375 MHz for ^{19}F) or a Bruker DPX-500 instrument (operating at 500 MHz for ^{1}H and 125 MHz for ^{13}C). Tetramethylsilane (TMS) served as the internal standard (0 ppm) for ^{1}H NMR, $CDCl_3$ was used as the internal standard (77.0 ppm) for ^{13}C NMR, and trifluorotoluene served as the internal standard (0 ppm) for ^{19}F NMR. Column chromatography purification was carried out using AMD Silica Gel 60 Å 230-400 mesh. Thin Layer Chromatography (TLC) was carried out using Merck Millipore TLC silica gel 60 F254 glass plates.

Protein Expression

Cloning of the Mb variants investigated in this work was described previously (Bordeaux *et al.*, *Angew. Chem. Int. Ed.* **2015,** *54*, 1744; Bajaj *et al.*, *Angew. Chem. Int. Ed.* **2016,** *55*, 16110). The Mb variants were expressed in *E. coli* BL21(DE3) or *E. coli* C41(DE3) cells as follows. After transformation, cells were grown in TB medium (ampicillin, 100 mg L^{-1}) at 37 °C (200 rpm) until OD_{600} reached 0.6. Cells were then induced with 0.25 mM isopropyl-β-D-1-thiogalactopyranoside (IPTG) and 0.3 mM δ-aminolevulinic acid (ALA). After induction, cultures were shaken at 180 rpm and 27 °C and harvested after 20 h by centrifugation at 4,000 rpm at 4 °C. Myoglobin concentration was determined after cell lysis by sonication, followed by CO-binding assay using an extinction coefficient ε_{415} = 187 $mM^{-1}cm^{-1}$.

Synthetic Procedures

Alkenes **7a-13b** were purchased from chemical suppliers and used without further purification. Alkene **14a** was synthesized as described previously.[2] Racemic standards for the stereoisomer analyses of the cyclopropane products **7b-14b** were prepared via cyclopropanation with Fe(III)TPPCl catalyst according to the general **Procedure A** provided below, which is based

on a published method by Morandi & Carreira (*Angew. Chem. Int. Ed.* **2010,** *49*, 938). Enantioenriched Mb-catalyzed cyclopropanation products were synthesized following **Procedure B**, and were used as authentic standards for the construction of calibration curves.

Chemical Synthesis of Racemic Standards for Cyclopropanation Products (Procedure A)

To a round bottom flask was added Fe(TPP)Cl (0.0066 mmol), 4-dimethylamino pyridine (DMAP) (0.022 mmol), sodium acetate (0.044 mmol), and trifluoroethylamine hydrochloride (0.33 mmol). Degassed distilled water (1 mL) and H_2SO_4 (1.2 μL, 0.022 mmol) were added, and the solution was degassed for one minute by sparging with argon. The alkene (0.22 mmol) was subsequently added, and a $NaNO_2$ solution (27 mg, 0.399 mmol, in 1 mL of degassed, distilled water) was added via syringe pump over 10 hours. After additional 4 hours, CH_2Cl_2 and water were added, and the aqueous phase was extracted with CH_2Cl_2 three times. The organic layer was collected, dried with $MgSO_4$, and concentrated under reduced pressure. Analysis of the products was performed by filtering the crude reaction mixture through a plug of silica and eluting with pentanes for chiral GC analysis. The cyclopropanation products consist of a racemic mixture of *trans-(S,S)* and *trans-(R,R)* isomers.

Whole-cell Cyclopropanation Reactions with *ex situ* generated DTE (Procedure B)

Whole-cell experiments were carried out at a 20 mL-scale using 19 mL of *E. coli* cells expressing Mb(H64V,V68A), 7.5 mM alkene, and 5 equivalents of EDA or DTE. In a typical procedure, alkene (0.15 mmol alkene in 1 mL of ethanol) was added slowly to a 125 mL Erlenmeyer flask containing a suspension of Mb(H64V,V68A)-expressing cells (OD_{600} = 40 in KPi, pH 7.2) under argon pressure, equipped with a magnetic stir bar and sealed with a rubber septum. The mixture was stirred at room temperature under argon pressure. In a 25 mL round-bottom flask containing a magnetic stir bar, either glycine ethyl ester hydrochloride or 2,2,2-trifluoroethylamine hydrochloride (0.75 mmol), sodium acetate (0.10 mmol), 4-dimethylaminopyridine (DMAP) (0.05 mmol) were added and dissolved in degassed, deionized water (8.00 mL). Then, sulfuric acid (0.05 mmol) was added and the solution was degassed for one minute by sparging with argon. A solution of sodium nitrite (0.90 mmol) in degassed, deionized water (4 mL) was added by syringe pump over 3-4 hours at room temperature. The generated diazo reagent (EDA or TDE) was gradually bubbled into the alkene and whole cell

reaction mixture using a continuous flow of argon. The reaction mixture was stirred for 4-12 hours at room temperature under anaerobic conditions. The TON for the whole-cell reactions were calculated based on Mb concentration in the reaction mixture as measured via UV-vis spectroscopy (ε_{415} = 187 $mM^{-1}cm^{-1}$) after cell lysis. The reaction mixture was extracted using diethyl ether (20 mL x 3) in 50-mL Falcon tubes. The tubes were shaken for 3 min manually, followed by additional vortexing for 3 min, and centrifugation (4,000 rpm, 15 min). The combined organic layers were dried over sodium sulfate and concentrated under reduced pressure in an ice-cold water bath. The crude product was purified via column chromatography using silica gel and 0-5% diethyl ether/pentanes as the eluent, keeping fractions on ice to prevent evaporation of the volatile products. Solvent was then removed by rotary evaporation using an ice-cold water bath to afford the desired product, which was characterized by GC-MS, ^{1}H-NMR, ^{13}C-NMR, and ^{19}F-NMR.

Product Analysis

The reactions were analyzed by adding 20 μL of internal standard (benzodioxole, 100 mM in methanol) to a 400 μL aliquot of the whole-cell reaction mixture, followed by extraction with 400 μL of dichloromethane (DCM) and centrifugation at 14,000 rpm. The organic layer was collected and analyzed by GC-FID (see **Analytical Methods** section for details on GC analyses). Calibration curves for the different cyclopropane products were constructed using pure products isolated from the whole-cell cyclopropanation reactions as references (see **Synthetic Procedures**). All measurements were performed at least in duplicate. For stereoselectivity determination, the samples were analyzed by GC-FID or SFC using a chiral column as described below.

Analytical Methods

Gas chromatography (GC) analyses were carried out using a Shimadzu GC-2010 gas chromatograph equipped with a FID detector, and a Cyclosil-B column (30 m x 0.25 mm x 0.25 μm film). The following GC method was used for TON analysis and stereoisomer separation for **7b-c** through **12b-c** and **14b-c**: 1 μL injection, injector temp.: 200 ºC, detector temp: 300 ºC. Gradient: column temperature set at 120ºC for 3 min, then to 150 ºC at 0.8 ºC/min, then to 245 ºC at 25 ºC/min. Total run time was 46.30 min.

Product	t_R for (*1S,2S*) isomer (min)	t_R for (*1R,2R*) isomer (min)
7b/7c	10.64	10.86
8b/8c	16.77	17.22
9b/9c	12.20	12.50
10b/10c	41.31	41.55
11b/11c	5.63	5.76
12b/12c	5.62	5.76
14b/14c	4.65	4.84

Stereoisomer resolution for compounds **13b-c** was performed by Supercritical Fluid Chromatography (SFC) analysis, using a JASCO Analytical and Semi-Preparative SFC instrument equipped with a column oven (35 °C), photodiode array detector, a backpressure regulator (12.0 MPa), a carbon dioxide pump and a sample injection volume of 3 μL. Daicel Chiralpak IA, IB or IC column (0.46 cm ID × 25 cm L) were used for separation of enantiomers. All samples were eluted using an isocratic solvent system with the indicated modifier (see table below) in liquid CO_2 at an elution rate of 4 mL/min and detected at λ = 220 nm. Total run time was 10.2 min.

Product	Column	Modifier Solvent	t_R for (*1S,2S*) isomer (min)	t_R for (*1R,2R*) isomer (min)
13b/13c	IB	Hexanes	3.77	3.35

Preparative Scale Cyclopropanation Reaction with *ex situ* Generated DTE (Procedure C)

A preparative scale experiment was carried out using 39 mL of *E. coli* cells expressing Mb(H64V,V68A), 30 mM alkene, and 10 equivalents of DTE. Alkene (0.600 mmol 4-methoxy styrene in 1 mL of ethanol) was added slowly to a 125 mL Erlenmeyer flask containing 39 mL of resuspended Mb(H64V,V68A)-expressing cells (OD_{600} = 80 in KPi, pH 7.2) under argon pressure, equipped with a magnetic stir bar and sealed with a rubber septum. The mixture was stirred at room temperature under argon pressure. A second 125 mL Erlenmeyer flask containing 20 mL of cell suspension and a magnetic stir bar was connected in tandem to the reaction flask. In a 50 mL round-bottom flask containing a magnetic stir bar, 2,2,2-trifluoroethylamine hydrochloride (6.00 mmol), sodium acetate (0.798 mmol), 4-dimethylaminopyridine (DMAP) (0.402 mmol) were

added and dissolved in degassed, deionized water (12.00 mL). Then, sulfuric acid (0.402 mmol) was added and the solution was degassed for one minute by sparging with argon. A solution of (7.20 mmol) sodium nitrite in degassed, deionized water (8 mL) was added by syringe pump over 4 hours at room temperature. The generated DTE was gradually bubbled into the alkene and whole cell reaction mixture using a continuous flow of argon. The reaction mixture was stirred for 5 hours at room temperature under anaerobic conditions. Reaction mixtures from both flasks were combined and extracted with dichloromethane (20 mL x 3). The organic layers were combined and dried over sodium sulfate. Dichloromethane was removed by distillation using a Liebig condenser at 50 °C. The concentrated crude product was transferred to a 250 mL round-bottom flask and a magnetic stir bar was added. Anhydrous dichloromethane (20 mL) was added and the mixture was allowed to stir at 0 °C. Then, *meta*-chloroperoxybenzoic acid (mCPBA) (0.1151 g, 0.667 mmol) was added and the reaction mixture was stirred overnight. After 12 h, residual alkene was consumed, as verified by TLC (1% diethyl ether/pentanes, visualized with CAN stain). The reaction mixture was washed with 5% aqueous KOH (20 mL) and extracted with dicholoromethane (15 mL x 3). Dichloromethane was removed by distillation and the product was purified via flash column chromatography using silica and 5% diethyl ether/pentanes to afford the cyclopropanation product as a clear, colorless oil (98.0 mg, 76% isolated yield, >99.9 de_{trans}, >99.9 $ee_{(1S,2S)}$).

Compound Characterization Data

1-Chloro-4-(2-(trifluoromethyl)cyclopropyl)benzene (7b):

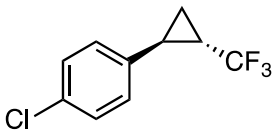

Following standard procedure **B,** except an additional 125 mL Erlenmeyer flask containing 20 mL of cell suspension was connected in tandem to the alkene and whole-cell reaction flask. Enantioenriched *trans* isomer 1-chloro-4-(2-(trifluoromethyl) cyclopropyl) benzene was isolated via column chromatography using silica and 100% pentanes to afford the product as a colorless oil, 67% yield. GC-MS m/z (% relative intensity): 222(13.4), 220(40.3), 185(100), 165(67.8), 151(47.6), 116(64.8), 115(82.9); ^{1}H-NMR (500 MHz, $CDCl_3$): δ 7.24 (d, J = 8.5 Hz, 2H), 7.03 (d, J = 8.5 Hz, 2H), 2.32 (dt, J = 10.0, 5.4 Hz, 1H), 1.77-1.70 (m, 1H), 1.37 (dt, 10.9, 5.6 Hz, 1H), 1.12-1.09 (m, 1H); ^{13}C NMR ($CDCl_3$, 100 MHz): δ 137.5, 132.6, 128.7, 127.9, 124.6, 23.4 (q, J = 37 Hz), 19.1, 10.8 (d, J = 2 Hz); ^{19}F NMR (375 MHz, $CDCl_3$): δ -4.5 (d, J = 2 Hz).

1-Bromo-4-(2-(trifluoromethyl)cyclopropyl)benzene (8b)

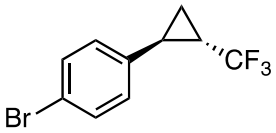

Following standard procedure **B,** except Mb(H64V,V68A)-expressing cells diluted to OD_{600} = 80 (KPi, pH 7.2) were used and an additional 125 mL Erlenmeyer flask containing 20 mL of cell suspension was connected in tandem to the alkene and whole-cell reaction flask. Enantioenriched *trans* isomer 1-bromo-4-(2-(trifluoromethyl)cyclopropyl)benzene was isolated via column chromatography using silica and 100% pentanes to afford the product as a colorless oil, 68% yield. GC-MS m/z (% relative intensity): 266(39.2), 264(41.6), 185(65.8), 165(62.0), 116(100), 115(63.6); ^{1}H-NMR (500 MHz, $CDCl_3$): δ 7.39 (d, J = 8.5 Hz, 2H), 6.97 (d, J = 8.4 Hz, 2H), 2.30 (dt, J = 10.1, 5.5 Hz, 1H), 1.77-1.70 (m, 1H), 1.37 (dt, J = 9.8, 5.7 Hz, 1H), 1.13-1.09 (m, 1H); ^{13}C-NMR (125 MHz, $CDCl_3$): δ 138.0, 131.7, 128.3, 124.6, 120.5, 23.4 (q, J = 37 Hz), 19.1 (d, J = 2 Hz), 10.8 (d, J = 2 Hz) ; ^{19}F NMR (375 MHz, $CDCl_3$): δ -4.5 (d, J = 2 Hz).

1-Methoxy-4-(2-(trifluoromethyl)cyclopropyl)benzene (9b):

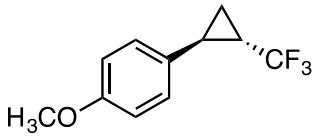

Following standard procedure **C,** enantioenriched *trans* isomer 1-methoxy-4-(2-(trifluoromethyl) cyclopropyl)benzene was isolated via flash column chromatography using silica and 5% diethyl ether in pentanes to afford the product as a colorless oil, 76% yield. GC-MS m/z (% relative intensity): 216(100), 215(45.4), 185(12.6), 147(70.5), 115(20.4); ^{1}H-NMR (500 MHz, $CDCl_3$): δ 7.08 (d, *J* = 10.6 Hz, 2H), 6.86 (d, *J* = 10.5 Hz, 2H), 3.80 (s, 3H), 2.35 (dt, *J* = 16.0, 8.5 Hz, 1H), 1.76-1.70 (m, 1H), 1.35 (dt, *J* = 13.0, 6.5 Hz, 1H), 1.14-1.05 (m, 1H); ^{13}C NMR ($CDCl_3$, 125 MHz): δ 158.5, 131.0, 127.4 (q, *J* = 338 Hz), 114.0, 53.3, 29.7, 23.0 (q, *J* = 36), 18.9, 10.4; ^{19}F NMR (375 MHz, $CDCl_3$): δ -4.4 (d, *J* = 6.8 Hz).

1-Nitro-4-(2-(trifluoromethyl)cyclopropyl)benzene (10b)

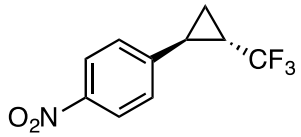

Following procedure **B**, enantioenriched *trans* isomer 1-nitro-4-(2-(trifluoromethyl) cyclopropyl)benzene was isolated via column chromatography using silica gel and 5% diethyl ether in pentanes to afford the product as a white crystalline solid, 43% yield. GC-MS m/z (% relative intensity): 231(80.5), 201(32.5), 165(43.3), 164(43.6), 145(34.4), 116(68.9), 115(100); ^{1}H-NMR (500 MHz, $CDCl_3$): δ 8.14 (d, *J* = 8.5 Hz, 2H), 7.22 (d, *J* = 8.6 Hz, 2H), 2.42 (dt, *J* = 15.0, 5.5 Hz, 1H), 1.92 (m, 1H), 1.50 (dt, *J* = 12.0, 5.9 Hz, 1H), 1.29 (m, 1H); ^{13}C NMR ($CDCl_3$, 125 MHz): δ 146.9 (d, *J* = 55 Hz), 127.1, 126.4, 124.2, 123.8, 58.3, 24.3 (q, *J* = 37 Hz), 19.5 (d, *J* = 3 Hz) , 18.4, 11.8 (d, *J* = 2 Hz); ^{19}F NMR (375 MHz, $CDCl_3$): δ -4.4 (d, *J* = 6.8 Hz).

1-Methyl-4-(2-(trifluoromethyl)cyclopropyl)benzene (11b)

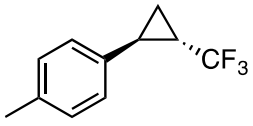

Following procedure **B,** except Mb(H64V,V68G)-expressing cells (OD_{600} = 80 in KPi, pH 7.2) were used and an additional 125 mL Erlenmeyer flask containing 20 mL of cell suspension was

connected in tandem to the alkene and whole-cell reaction flask. Enantioenriched *trans* isomer 1-methyl-4-(2-(trifluoromethyl)cyclopropyl)benzene was isolated via column chromatography using silica gel and 100% pentanes to afford the product as a colorless oil, 78% yield. GC-MS m/z (% relative intensity): 200(77.3), 185(58.2), 165(33.1), 131(100), 116(30.5), 115(38.3), 91(27.1); ^{1}H-NMR (500 MHz, $CDCl_3$): δ 7.08 (d, J = 8.0 Hz, 2H), 6.99 (d, J = 7.5, 2H), 2.31 (m, 4H), 1.76 (m, 1H), 1.32 (dt, J = 15.0, 5.5 Hz, 1H), 1.12-1.08 (m, 1H); ^{13}C NMR ($CDCl_3$, 125 MHz): δ 136.4, 136.0, 129.3, 126.4, 124.9, 23.2 (q, J = 36 Hz), 21.0, 19.2, 10.7 (d, J = 2.1); ^{19}F NMR (375 MHz, $CDCl_3$): δ -4.3 (d, J = 6.4 Hz).

1-Methyl-3-(2-(trifluoromethyl)cyclopropyl)benzene (12b)

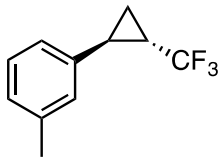

Following procedure **B,** except Mb(H64V,V68G)-expressing cells (OD_{600} = 80 in KPi, pH 7.2) were used and an additional 125 mL Erlenmeyer flask containing 20 mL of cell suspension was connected in tandem to the alkene and whole-cell reaction flask. Enantioenriched *trans* isomer 1-methyl-3-(2-(trifluoromethyl)cyclopropyl)benzene was isolated via column chromatography using silica gel and 100% pentanes to afford the product as a colorless oil, 82% yield. GC-MS m/z (% relative intensity): 200(74.7), 185(47.2), 165(31.8), 131(100), 116(29.9), 115(36.9), 91(26.5); ^{1}H-NMR (500 MHz, $CDCl_3$): δ 7.17-7.14 (t, J = 7.5 Hz, 1H), 7.01 (d, J = 7.5 Hz, 1H), 6.91 (s, 1H), 6.90-6.87 (m, 2H), 2.30 (m, 4H), 1.80 (m, 1H), 1.33 (dt, J = 15 Hz, 5 Hz, 1H), 1.14-1.10 (m, 1H); ^{13}C NMR ($CDCl_3$, 125 MHz): δ 139.0, 138.3, 128.5, 127.5, 127.3, 127.0 123.4, 23.3 (q, 37 Hz), 21.4, 19.5, 10.8; ^{19}F NMR (375 MHz, $CDCl_3$): δ -4.4 (d, J = 6.4 Hz).

1-(2-(Trifluoromethyl)cyclopropyl)naphthalene (13b)

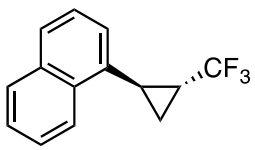

Following procedure **B**, except Mb(H64V,V68A)-expressing cells (OD_{600} = 80 in KPi, pH 7.2) were used. Enantioenriched *trans* isomer 1-(2-(Trifluoromethyl)cyclopropyl) naphthalene was isolated via column chromatography using silica gel and 100% pentanes to afford the product as a

colorless oil, 58% yield. GC-MS m/z (% relative intensity): 236(86.4), 167(100), 165(57.0), 153(44.3), 152(49.9), 139(20.8); ^{1}H-NMR (500 MHz, $CDCl_3$): δ 8.29 (d, *J* = 8 Hz, 1H), 7.86-7.75 (dd, *J* = 40, 8 Hz, 2H), 7.59-7.49 (dt, *J* = 25, 7 Hz, 2H), 7.40 (t, *J* = 7.2 Hz, 1H), 7.27 (d, *J* = 6.9 Hz, 1H), 2.82-2.77 (m, 1H), 1.86-1.80 (m, 1H), 1.52-1.47 (m, 1H), 1.32 (dt, *J* = 13.0, 6.3 Hz, 1H); ^{13}C NMR ($CDCl_3$, 125 MHz): δ 134.6, 133.6, 132.9, 128.6, 127.9, 127.5, 126.4, 126.0, 125.3, 124.5, 123.8, 21.0 (q, *J* = 73, 36 Hz), 17.9 (d, *J* = 2 Hz), 9.1 (d, *J* = 2 Hz); ^{19}F NMR (375 MHz, $CDCl_3$): δ -3.8 (d, *J* = 6.4 Hz).

3-(1-Methyl-2-(trifluoromethyl)cyclopropyl)thiophene (14b)

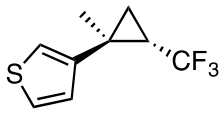

Following procedure **B**, except Mb(H64V,V68A)-expressing cells (OD_{600} = 80 in KPi, pH 7.2) were used and an additional 125 mL Erlenmeyer flask containing 20 mL of cell suspension was connected in tandem to the alkene and whole-cell reaction flask. Enantioenriched *trans* isomer 3-(1-methyl-2-(trifluoromethyl)cyclopropyl)thiophene was isolated via column chromatography using silica gel and 100% pentanes to afford the product as a colorless oil, 71% yield. GC-MS m/z (% relative intensity): 206(86.8), 191(100), 137(63.1), 97(18.4); ^{1}H-NMR (400 MHz, $CDCl_3$): δ 7.22 (s, 2H), 6.97 (s, 1H), 6.87 (d, J = 4.9 Hz, 1H), 1.78-1.68 (m, 1H), 1.53 (s, 3H), 1.33-1.31 (m, 1H), 1.22 (m, 1H); ^{13}C NMR ($CDCl_3$, 100 MHz): δ 127.4, 126.2, 125.7, 119.8, 29.7, 27.4 (q, *J* = 51, 29 Hz), 18.9, 18.1 (d, *J* = 2 Hz); ^{19}F NMR (375 MHz, $CDCl_3$): δ 2.6 (d, *J* = 7.6 Hz).

X-ray crystallographic analyses

A crystal (0.055 x 0.081 x 0.104 mm^3) was attached to a nylon loop and mounted on a Rigaku Oxford Diffraction XtaLAB Synergy four-circle diffractometer equipped with a HyPix-6000HE area detector for data collection at 100 K (Rigaku Oxford Diffraction. *CrysAlisPro Software system*, version 1.171.39.7f; Rigaku Corporation: Oxford, UK, 2015). A preliminary set of cell constants and an orientation matrix were calculated from reflections harvested from a sampling of reciprocal space. Full data collections were carried out using CuKα radiation (1.54184 Å, PhotonJet-S Cu 50W Microfocus) with frame times ranging from three to seven seconds, frame widths of 0.5 degrees, and a detector distance of approximately four cm. The intensity data were scaled and corrected for absorption, and final cell constants were calculated from the xyz centroids of strong reflections from the actual data collections after integration. Space group $P2_1$ was determined based on systematic absences and intensity statistics. Structures were solved using SHELXT (Sheldrick, G. M. *SHELXT*, version 2014/5; University of Göttingen: Göttingen, Germany) and refined using SHELXL (against F^2) (Sheldrick, G. M. *SHELXL-2016/6*; *Acta Crystallogr.* **2015**, *C71*, 3-8.). All non-hydrogen atoms were refined with anisotropic displacement parameters. All hydrogen atoms were placed in ideal positions and refined as riding atoms with relative isotropic displacement parameters. The final full matrix least squares refinement converged to $R1$ = 0.0294 (F^2, $I > 2\sigma(I)$) and $wR2$ = 0.0796 (F^2, all data). The absolute configuration was determined by anomalous dispersion effects (Parsons, S; Flack, H. D.; Wagner, T. *Acta Crystallogr.* **2013**, *B69*, 249-259).

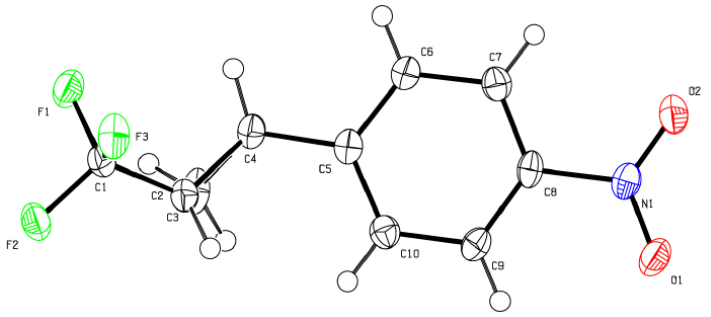

Figure S3. ORTEP of **10b** with ellipsoids drawn at the 50% probability level. Hydrogen atoms were located in the difference Fourier map and refined freely. They are represented here as spheres of arbitrary radius for clarity. Absolute configuration was determined by anomalous dispersion effects produced with CuKα radiation.

Table S3: Crystal data summary for **10b**.

Empirical Formula	$C_{10}H_8F_3NO_2$
FW	231.17
T (K)	100.0(1)
crystal system	monoclinic
space group	$P2_1$
a (Å)	8.0948(3)
b (Å)	6.72581(17)
c (Å)	9.5368(3)
β (deg)	110.999(4)
V (Å^3)	484.74(3)
Z	2
ρ_{calcd} (g cm^{-3})	1.584
μ (mm^{-1})	1.312
color, shape	colorless, plate
reflections collected	16801
reflections independent	1694
R_{int}[a]	0.0722
reflections observed	1645
number of parameters	145
GOF[b] on F^2	1.065
$R1$ [$I > 2\sigma(I)$][c]	0.0294
$wR2$[d]	0.0796

[a] $R_{int} = \Sigma\ |F_o^2 - \langle F_o^2 \rangle| / \Sigma\ F_o^2$. [b] GOF = $S = [\Sigma\ w(F_o^2 - F_c^2)^2 / (m - n)]^{1/2}$, where $w = 1 / [\sigma^2(F_o^2) + (aP)^2 + bP]$, $P = 1/3$ max $(0, F_o^2) + 2/3F_c^2$, m = number of independent reflections, and n = number of parameters. [c] $R1 = \Sigma\ ||F_o| - |F_c|| / \Sigma\ |F_o|$. [d] $wR2 = [\Sigma\ w(F_o^2 - F_c^2)^2 / \Sigma\ wF_o^2]^{1/2}$.

NMR Spectra

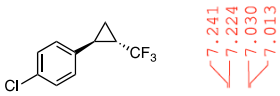
Cl
CF3

7.241
7.224
7.030
7.013


2.319
2.307
2.299
2.289
2.279
1.773
1.760
1.747
1.733
1.721
1.708
1.695
1.367
1.355
1.345
1.337
1.325
1.131
1.119
1.102
1.090

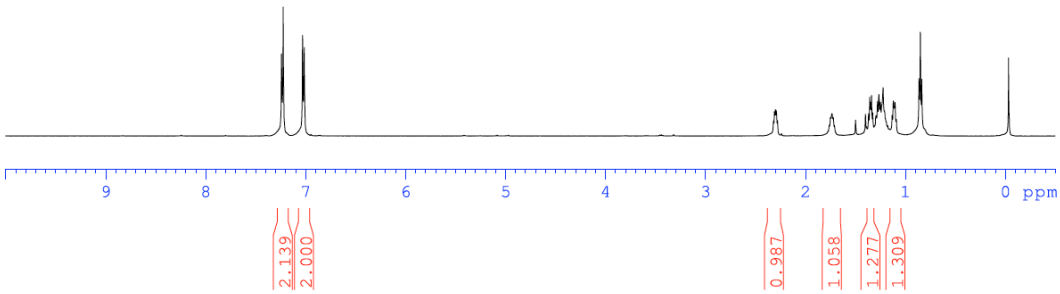
9
8
7
6
5
4
3
2
1
0 ppm
2.139
2.000
0.987
1.058
1.277
1.309

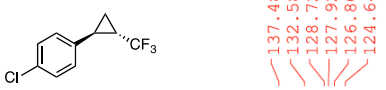
Cl
CF3

137.485
132.585
128.720
127.929
126.802
124.647


23.422
23.128
22.834
22.540
19.049
19.030
10.802
10.786

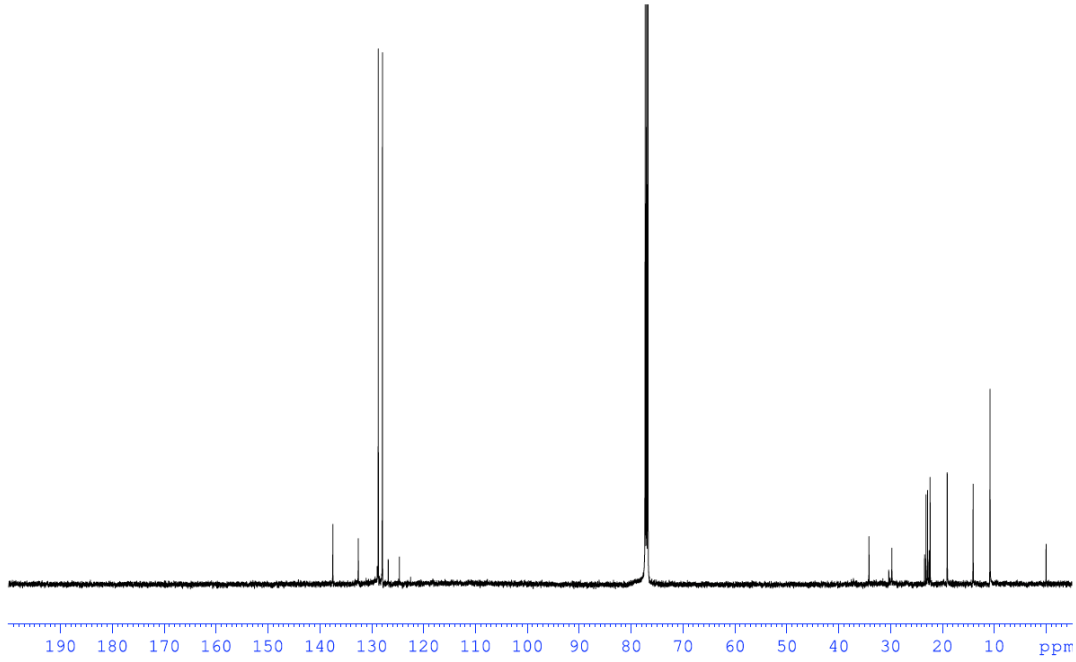
190
180
170
160
150
140
130
120
110
100
90
80
70
60
50
40
30
20
10
ppm

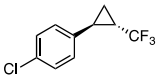
CF3
Cl

4.494
4.511
140 130 120 110 100 90 80 70 60 50 40 30 20 10 0 -10 -20 ppm

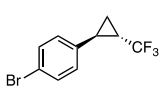
CF3
Br


7.392
7.375
6.972
6.955


2.304
2.293
2.284
2.274
2.263
1.774
1.761
1.750
1.743
1.736
1.734
1.727
1.722
1.721
1.709
1.696
1.368
1.357
1.349
1.346
1.338
1.327
1.131
1.119

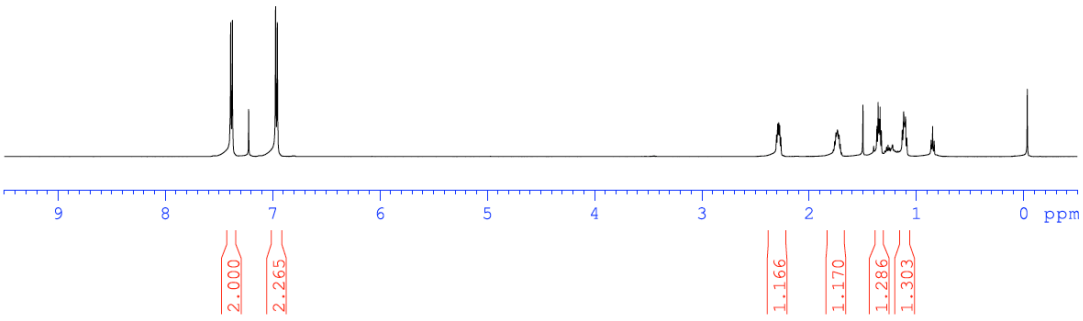
9 8 7 6 5 4 3 2 1 0 ppm
2.000
2.265
1.166
1.170
1.286
1.303

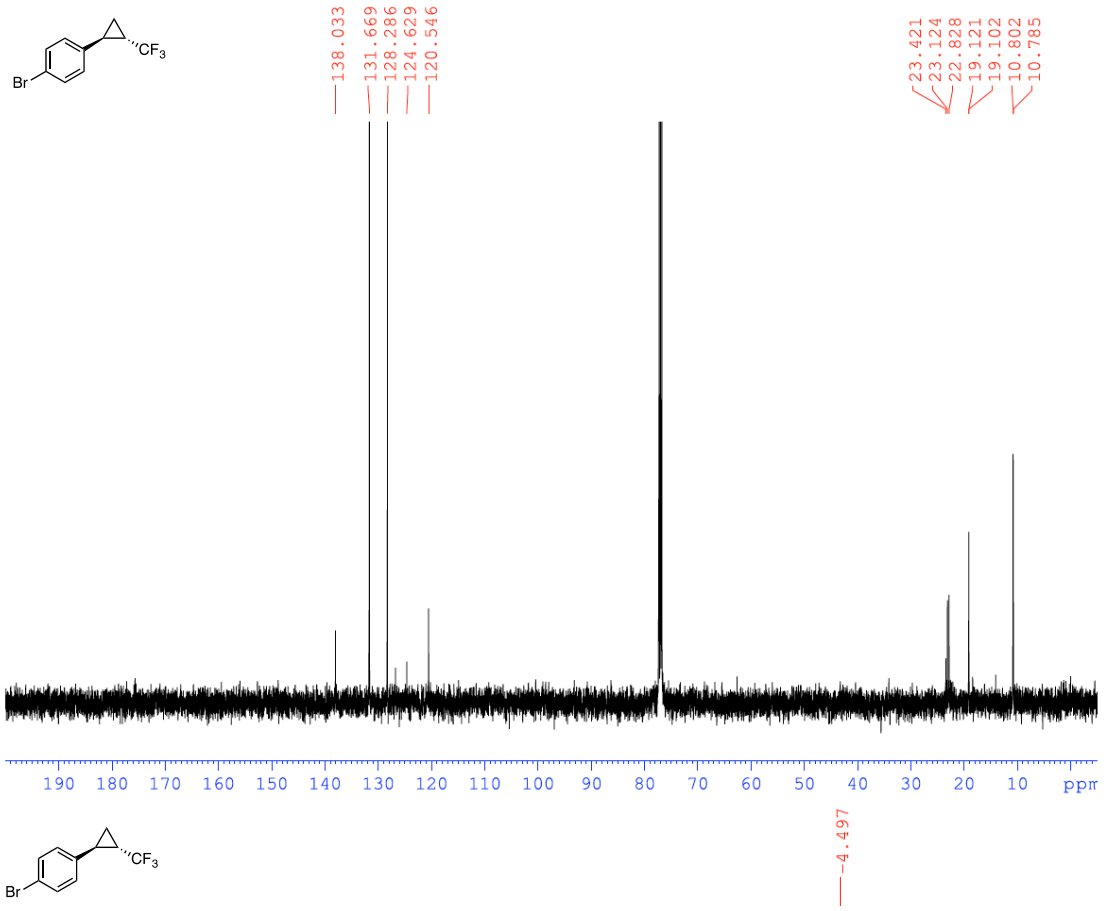
Br
CF3
138.033
131.669
128.286
124.629
120.546
23.421
23.124
22.828
19.121
19.102
10.802
10.785
190 180 170 160 150 140 130 120 110 100 90 80 70 60 50 40 30 20 10 ppm
Br
CF3
-4.497
90 80 70 60 50 40 30 20 10 0 -10 -20 ppm

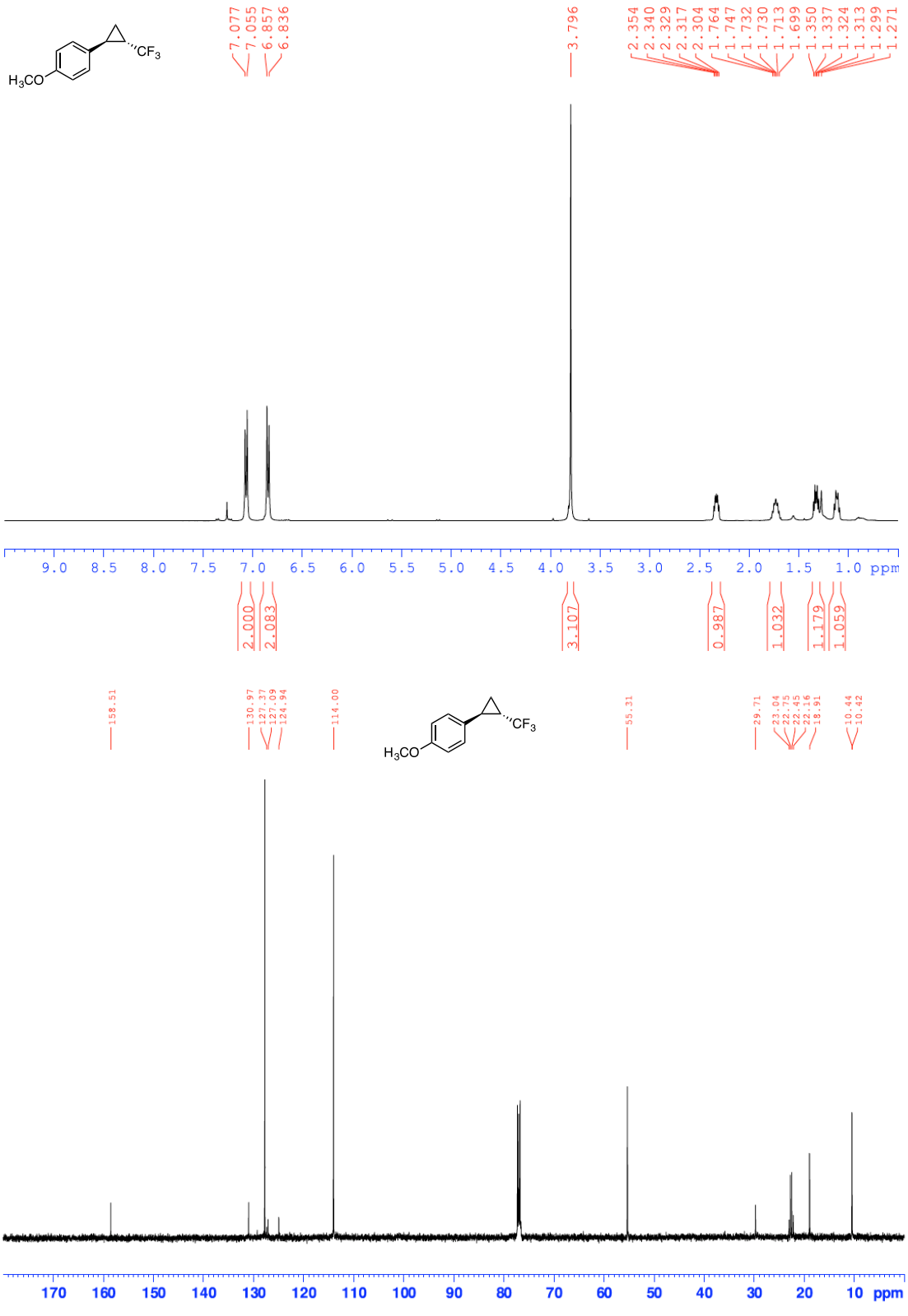
7.077
7.055
6.857
6.836
3.796
2.354
2.340
2.329
2.317
2.304
1.764
1.747
1.732
1.730
1.713
1.699
1.350
1.337
1.324
1.313
1.299
1.271
CF3
H3CO
9.0 8.5 8.0 7.5 7.0 6.5 6.0 5.5 5.0 4.5 4.0 3.5 3.0 2.5 2.0 1.5 1.0 ppm
2.000
2.083
3.107
0.987
1.032
1.179
1.059
158.51
130.97
127.37
127.09
124.94
114.00
55.31
29.71
23.04
22.75
22.45
22.16
18.91
10.44
10.42
170 160 150 140 130 120 110 100 90 80 70 60 50 40 30 20 10 ppm

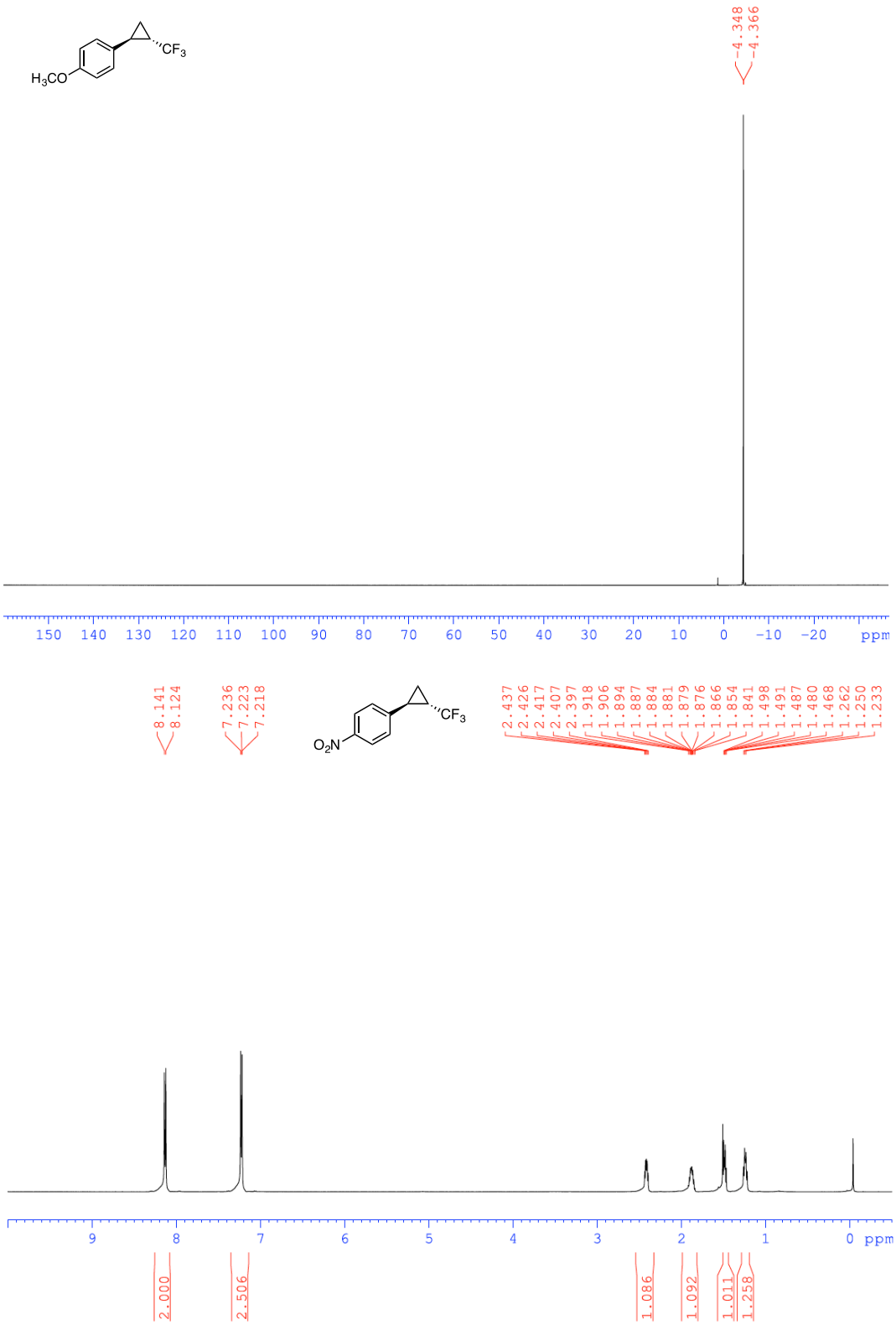
H3CO
CF3
4.348
4.366
150 140 130 120 110 100 90 80 70 60 50 40 30 20 10 0 -10 -20 ppm
8.141
8.124
7.236
7.223
7.218
O2N
CF3
2.437
2.426
2.417
2.407
2.397
1.918
1.906
1.894
1.887
1.884
1.881
1.879
1.876
1.866
1.854
1.841
1.498
1.491
1.487
1.480
1.468
1.262
1.250
1.233
9 8 7 6 5 4 3 2 1 0 ppm
2.000
2.506
1.086
1.092
1.011
1.258

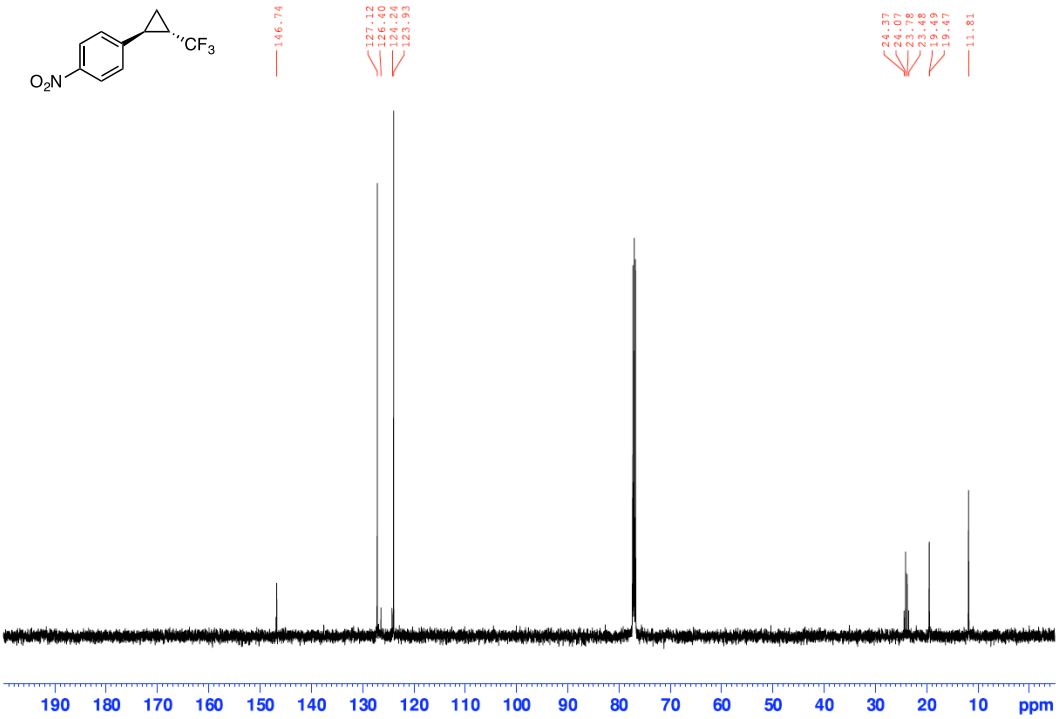
146.74
127.12
126.40
124.24
123.93
24.37
24.07
23.78
23.48
19.49
19.47
11.81
190 180 170 160 150 140 130 120 110 100 90 80 70 60 50 40 30 20 10 ppm

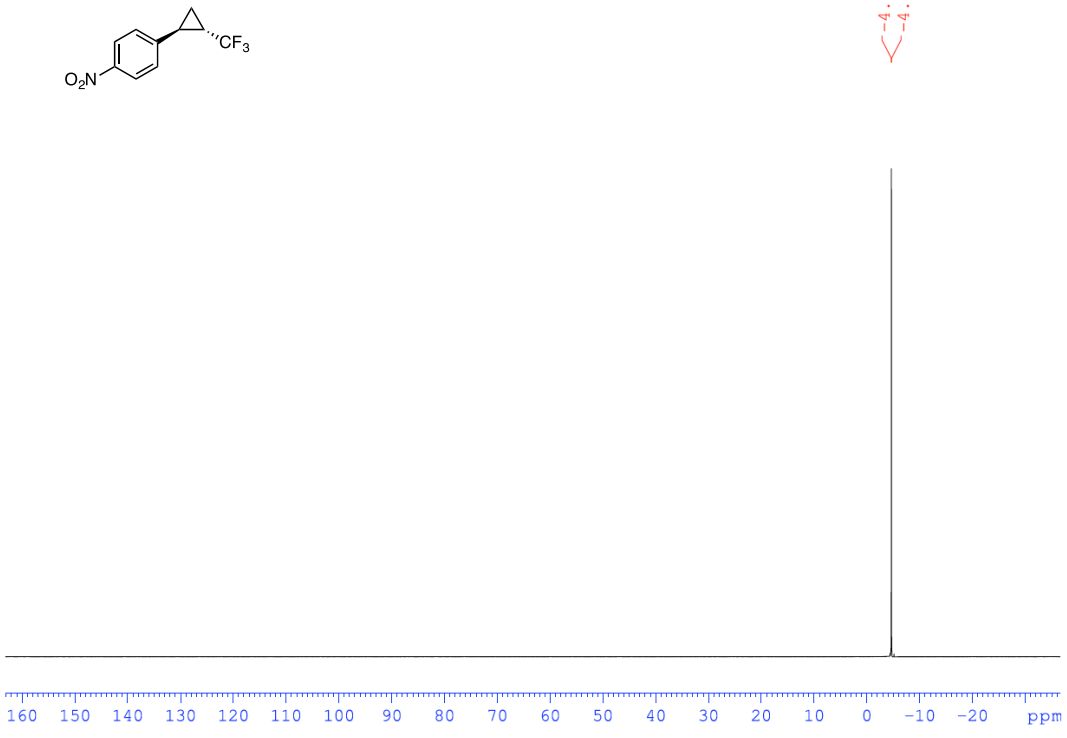
-4.643
-4.659
160 150 140 130 120 110 100 90 80 70 60 50 40 30 20 10 0 -10 -20 ppm

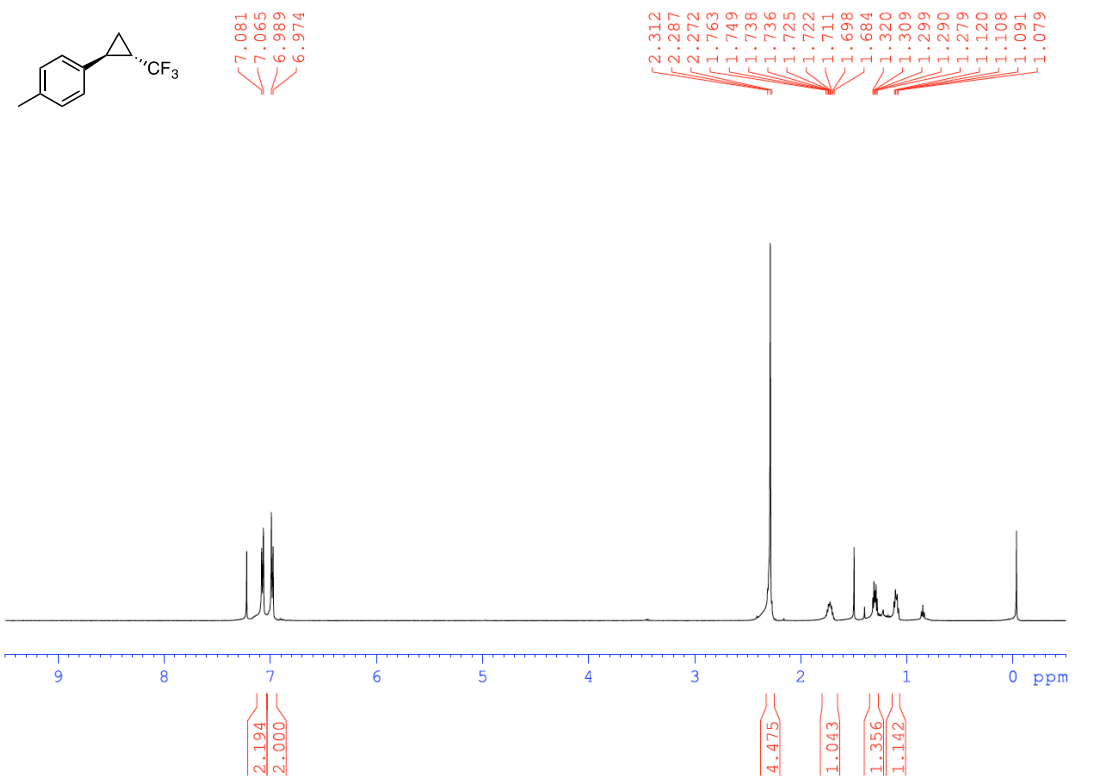
CF3
7.081
7.065
6.989
6.974
2.312
2.287
2.272
1.763
1.749
1.738
1.736
1.725
1.722
1.711
1.698
1.684
1.320
1.309
1.299
1.290
1.279
1.120
1.108
1.091
1.079
9
8
7
6
5
4
3
2
1
0 ppm
2.194
2.000
4.475
1.043
1.356
1.142

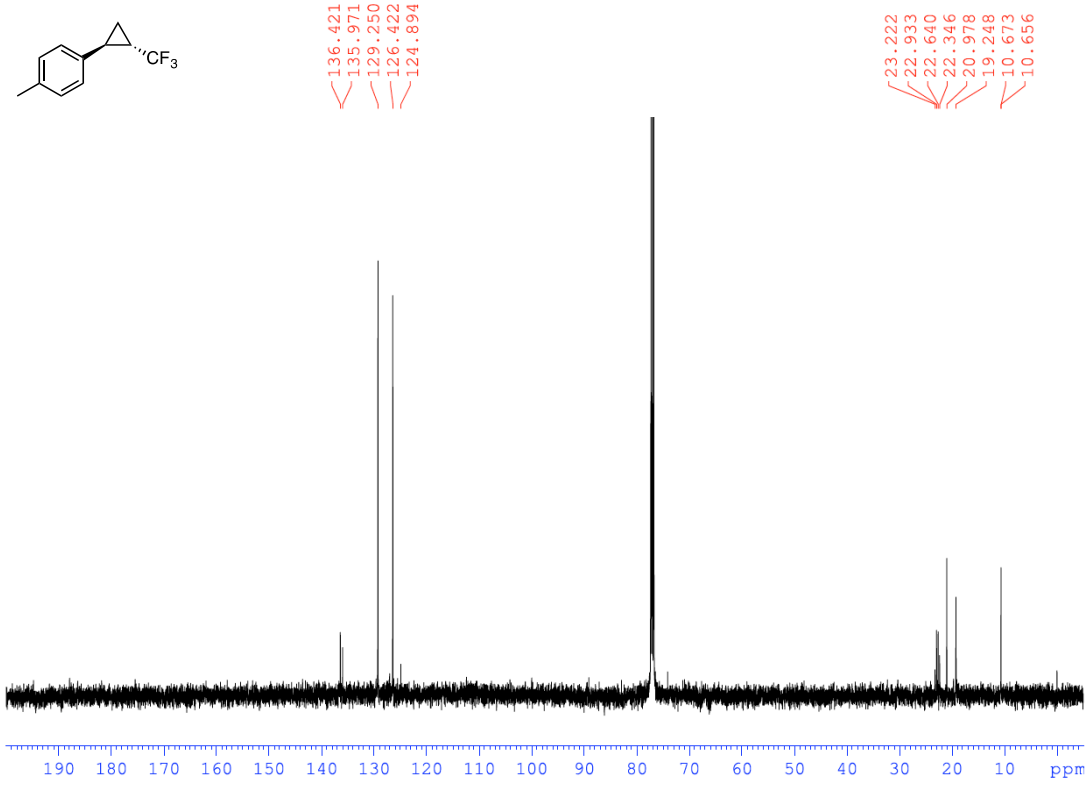
CF3
136.421
135.971
129.250
126.422
124.894
23.222
22.933
22.640
22.346
20.978
19.248
10.673
10.656
190
180
170
160
150
140
130
120
110
100
90
80
70
60
50
40
30
20
10
ppm

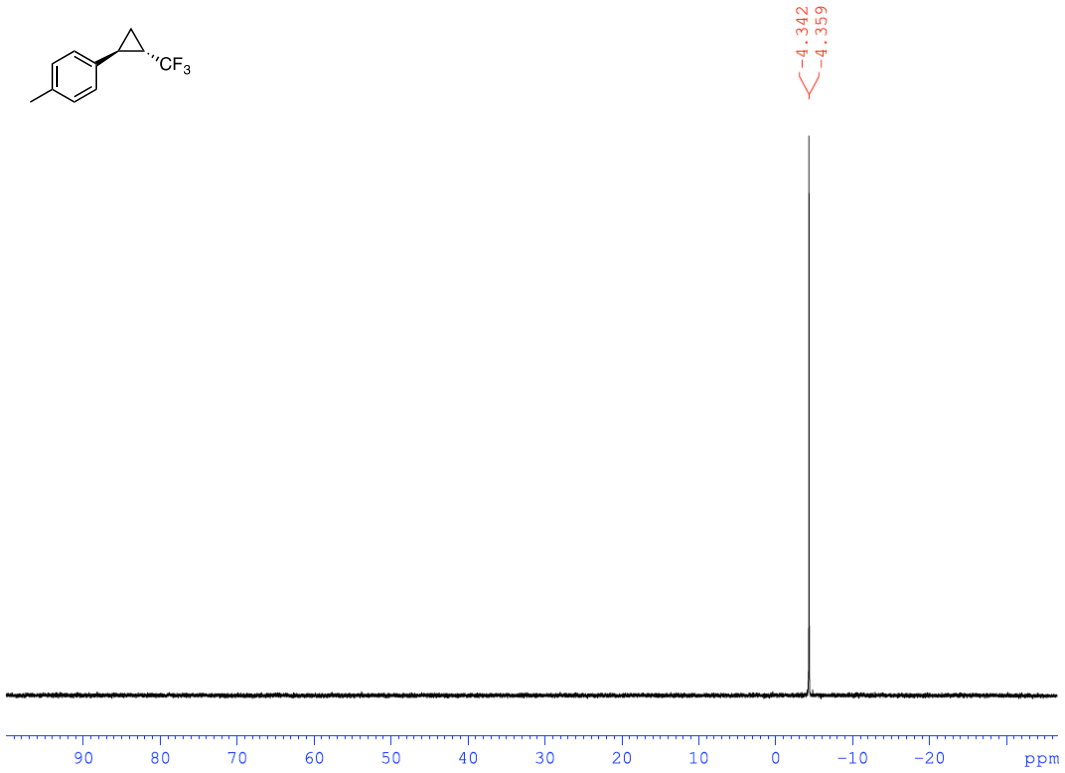
CF3
-4.342
-4.359
90
80
70
60
50
40
30
20
10
0
-10
-20
ppm

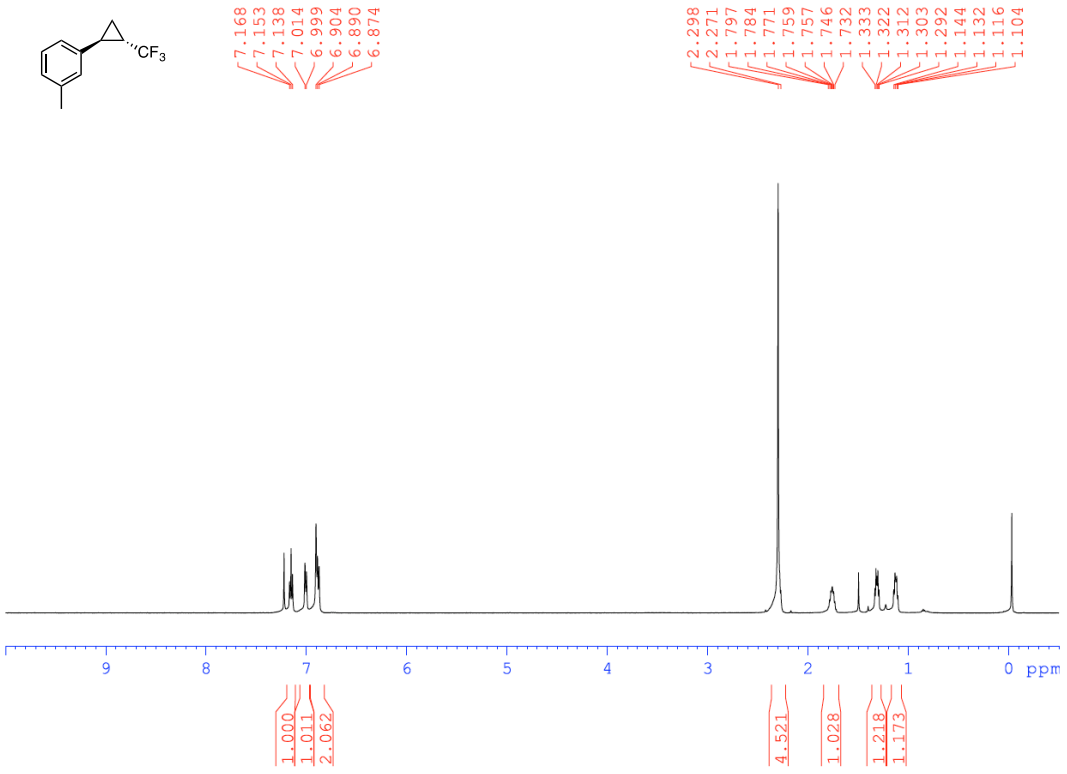
CF3
7.168
7.153
7.138
7.014
6.999
6.904
6.890
6.874
2.298
2.271
1.797
1.784
1.771
1.759
1.757
1.746
1.732
1.333
1.322
1.312
1.303
1.292
1.144
1.132
1.116
1.104
9
8
7
6
5
4
3
2
1
0 ppm
1.000
1.011
2.062
4.521
1.028
1.218
1.173

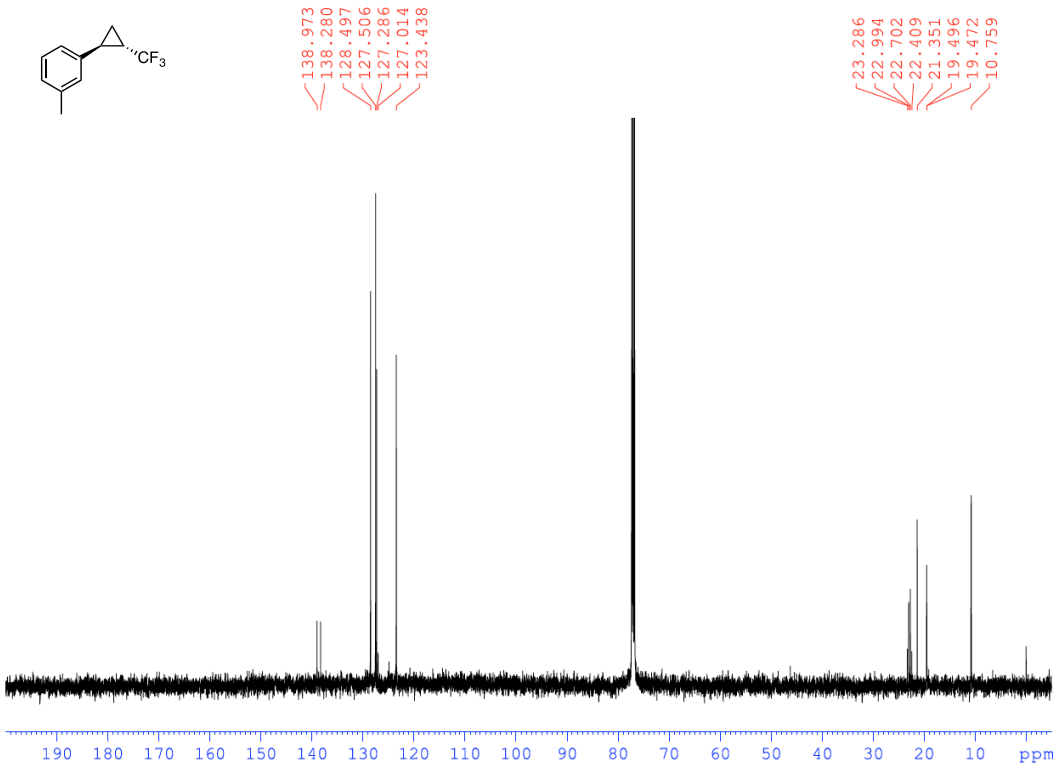
CF3
138.973
138.280
128.497
127.506
127.286
127.014
123.438
23.286
22.994
22.702
22.409
21.351
19.496
19.472
10.759
190 180 170 160 150 140 130 120 110 100 90 80 70 60 50 40 30 20 10 ppm

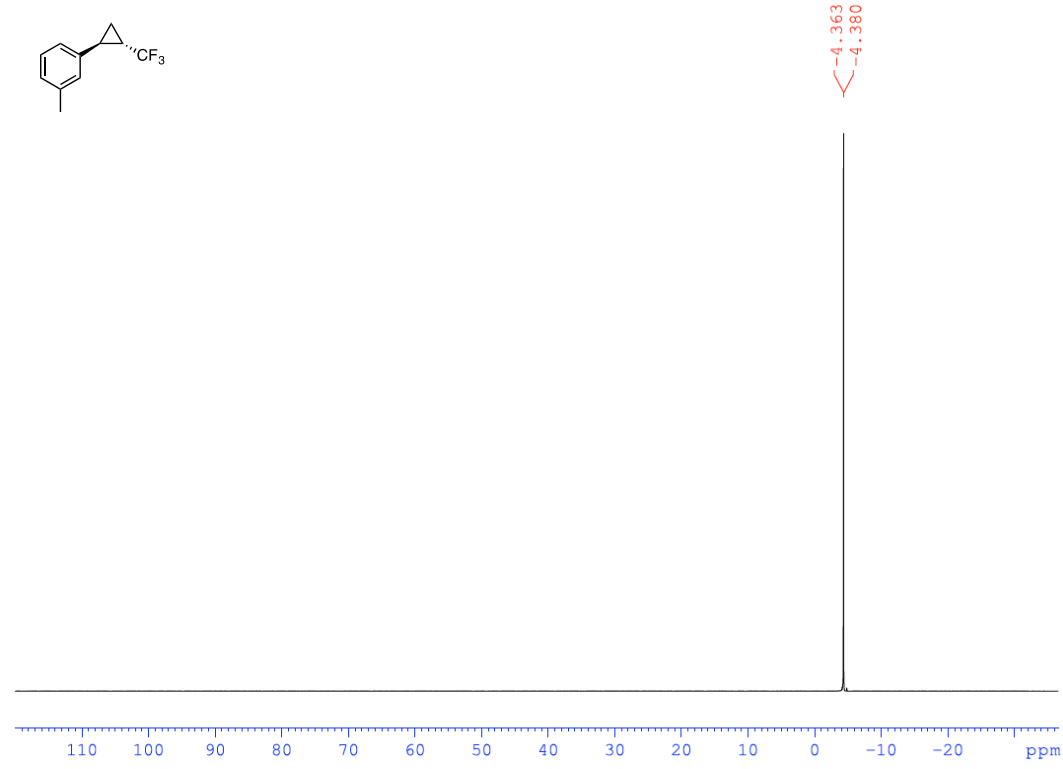
CF3
-4.363
-4.380
110 100 90 80 70 60 50 40 30 20 10 0 -10 -20 ppm

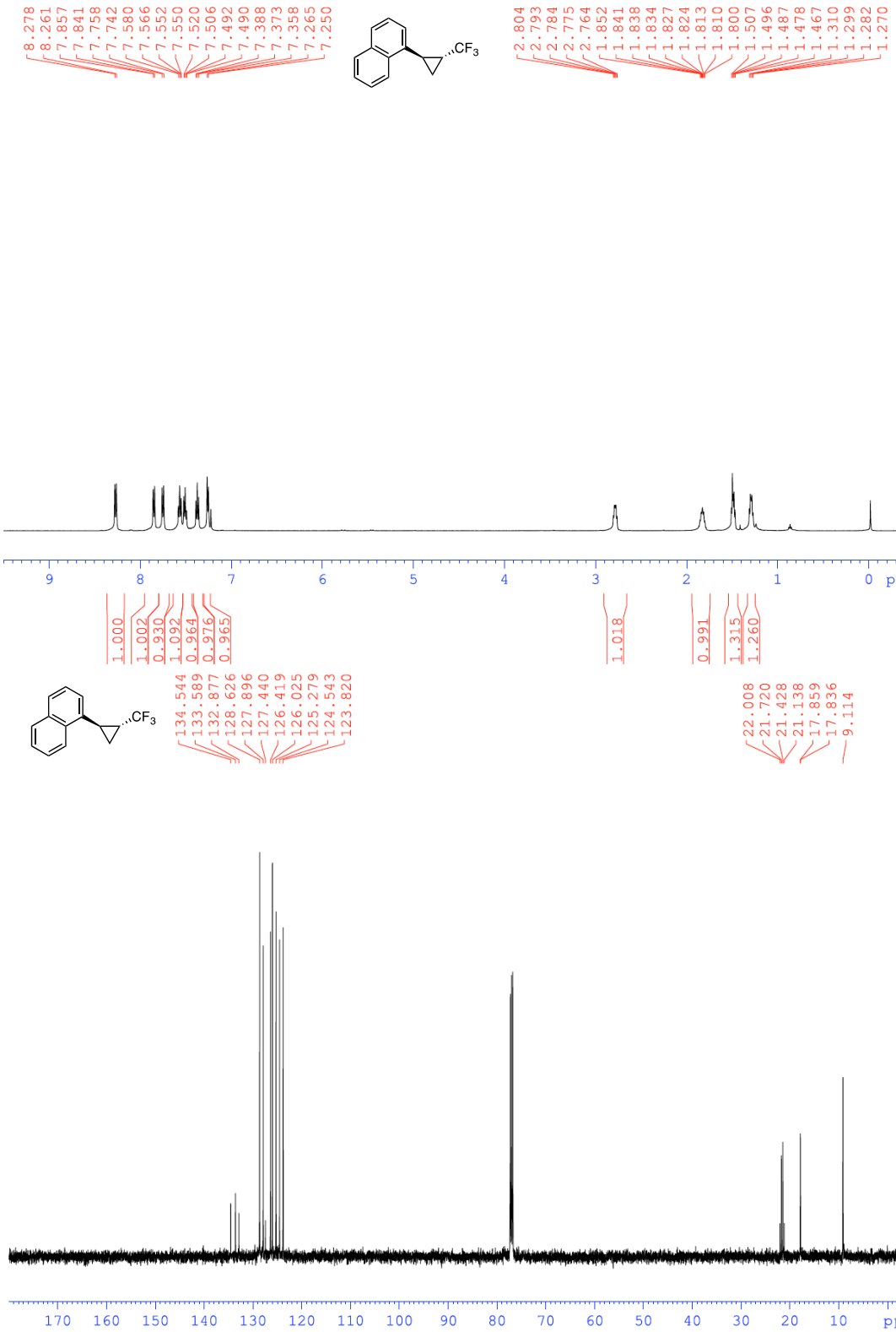
8.278
8.261
7.857
7.841
7.758
7.742
7.580
7.566
7.552
7.550
7.520
7.506
7.492
7.490
7.388
7.373
7.358
7.265
7.250
CF3
2.804
2.793
2.784
2.775
2.764
1.852
1.841
1.838
1.834
1.827
1.824
1.813
1.810
1.800
1.507
1.496
1.487
1.478
1.467
1.310
1.299
1.282
1.270
9 8 7 6 5 4 3 2 1 0 ppm
1.000
1.002
0.930
1.092
0.964
0.976
0.965
1.018
0.991
1.315
1.260
CF3
134.544
133.589
132.877
128.626
127.896
127.440
126.419
126.025
125.279
124.543
123.820
22.008
21.720
21.428
21.138
17.859
17.836
9.114
170 160 150 140 130 120 110 100 90 80 70 60 50 40 30 20 10 ppm

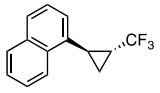
CF3

3.808
3.825
90
80
70
60
50
40
30
20
10
0
-10
-20
ppm

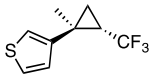
S
CF3


7.224
6.969
6.872
6.859


1.777
1.757
1.736
1.720
1.698
1.678
1.532
1.503
1.398
1.343
1.329
1.308
1.280
1.263

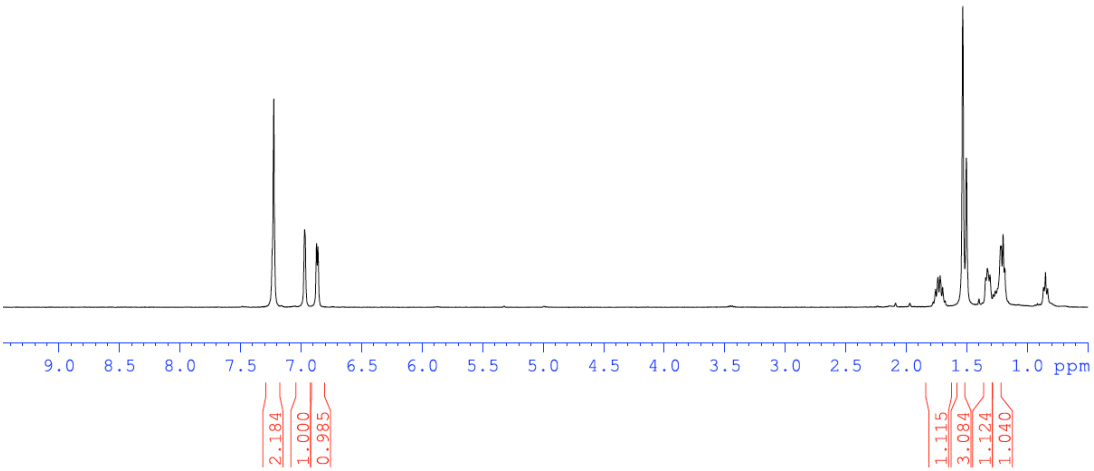
9.0
8.5
8.0
7.5
7.0
6.5
6.0
5.5
5.0
4.5
4.0
3.5
3.0
2.5
2.0
1.5
1.0 ppm
2.184
1.000
0.985
1.115
3.084
1.124
1.040

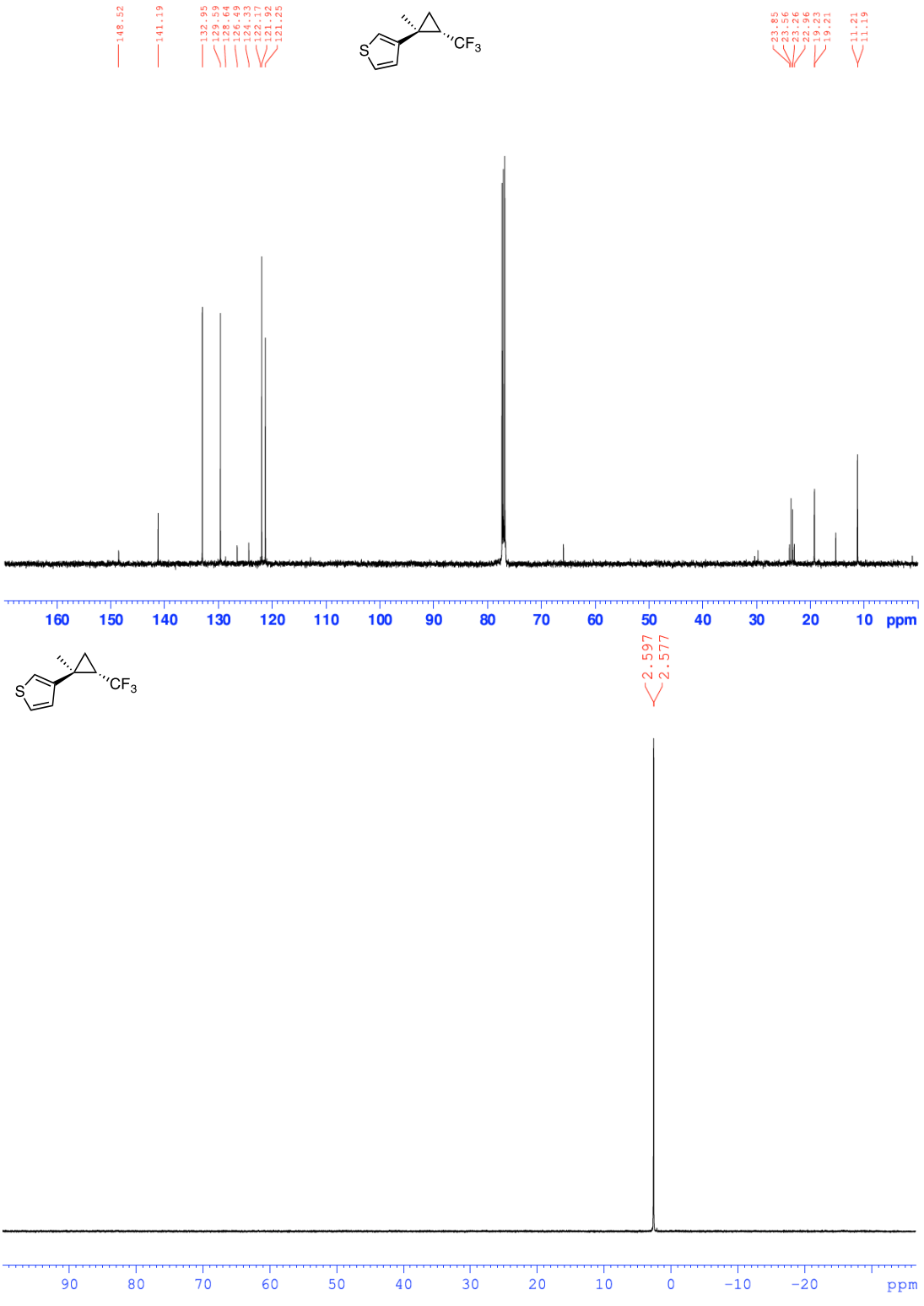
148.52
141.19
132.95
129.59
128.64
126.49
124.33
122.17
121.92
121.25
23.85
23.56
23.26
22.96
19.23
19.21
11.21
11.19
S
CF3
160
150
140
130
120
110
100
90
80
70
60
50
40
30
20
10
ppm
2.597
2.577
90
80
70
60
50
40
30
20
10
0
−10
−20
ppm